

Elastic Full Procrustes Analysis of Plane Curves via Hermitian Covariance Smoothing

BY A. STÖCKER, M. PFEUFFER, L. STEYER AND S. GREVEN

*Chair of Statistics, School of Business and Economics, Humboldt-Universität zu Berlin,
Unter den Linden 6, 10099 Berlin, Germany*

almond.stoecker@hu-berlin.de manuel.pfeuffer@esmt.org lisa.steyer@hu-berlin.de
sonja.greven@hu-berlin.de

SUMMARY

Determining the mean shape of a collection of curves is not a trivial task, in particular when curves are only irregularly/sparingly sampled at discrete points. We propose an elastic full Procrustes mean of shapes of (oriented) plane curves, which are considered equivalence classes of parameterized curves with respect to translation, rotation, scale, and re-parameterization (warping), based on the square-root-velocity framework. Identifying the real plane with the complex numbers, we establish a connection to covariance estimation in irregular/sparse functional data analysis and propose Hermitian covariance smoothing for (in)elastic full Procrustes mean estimation. We demonstrate the performance of the approach in a phonetic study on tongue shapes and in different realistic simulation settings, inter alia based on handwriting data.

Some key words: Complex Gaussian Process; Functional data; Principal component analysis; Shape analysis; Square-root-velocity.

1. INTRODUCTION

When comparing the shape of, say, a specific outline marked on medical images across different patients, the concrete coordinate system used for recording is often arbitrary and not of interest: the shape neither depends on positioning in space, nor on orientation or size. Analogously, the outline can be mathematically represented via a parameterized curve $\beta : [0, 1] \rightarrow \mathbb{R}^2$, but the particular parameterization of the outline curve is often not of interest. We study datasets where an observational unit is the shape of a plane curve, defined as equivalence class a) over the shape invariances translation, rotation and scale and b) over re-parameterization. More specifically, we generalize the notion of a full Procrustes mean from discrete landmark shape analysis (Dryden & Mardia, 2016) with invariances a) to this functional (curve) case, implying the alignment of the recorded data with respect to all involved invariances a) and b).

For landmark shapes (i.e. a)), different notions of mean shape are well-established including, in addition to the full Procrustes mean, in particular also the intrinsic shape mean, i.e. the Riemannian center of mass in the shape space. Dryden et al. (2014) discuss properties of different shape mean concepts, pointing out that the full Procrustes mean is more robust with respect to outliers than the intrinsic mean or the *partial* Procrustes mean fixing scale to unit size. Further discussion of these three mean concepts, which all present Fréchet means based on different distances, can be found in Huckemann (2012). The full Procrustes mean also arises as the mode (Dryden & Mardia, 2016) of a complex Bingham distribution (Kent, 1994) on (unit-norm) landmark configurations $\mathbf{X} \in \mathbb{C}^k$ of k landmarks, which is commonly used to model planar landmark

shapes, identifying the real plane $\mathbb{R}^2 \cong \mathbb{C}$ with the complex numbers. Moreover, it corresponds to the leading eigenvector of the complex covariance matrix of \mathbf{X} , an important point we generalize for the estimation strategy proposed for curve mean shapes in this paper.

Compared to landmark shapes, invariance with respect to re-parameterization (warping) b) poses an additional challenge in the analysis of curves, which is highly related to the registration problem in function data analysis (FDA, Ramsay & Silverman, 2005). In this context, Srivastava et al. (2011) propose an *elastic* re-parameterization invariant metric on curves, allowing to define a proper distance between two curves via optimal warping alignment. Greatly simplifying the formulation of the metric by working with square-root-velocity (SRV) transformations of the curves, their framework also allows incorporation of shape invariances a) along the lines of statistical shape analysis. This lead to a rapidly growing literature on *functional* shape analysis of curves in the SRV-framework (see e.g., Srivastava & Klassen, 2016). However, so far the focus lay on elastic generalization of the intrinsic shape mean instead of the (potentially more robust) full Procrustes mean.

Moreover, except for Steyer et al. (2021) considering only reparameterization invariance b), analysis of sparsely/irregularly observed curves in the SRV-framework has not yet been considered. Such data with a comparably low number of samples per curve often results in practice when the sampling rate of a measurement device is limited, or the resolution of images used for curve segmentation is coarse. In FDA (Ramsay & Silverman, 2005), sparse/irregular functional data is commonly distinguished from dense/regular data, as it requires explicit treatment. Models for sparse/irregular data are often based on smooth (spline) function bases and involve an assumption of (small) measurement errors on the discrete curve evaluations as common in practice (Greven & Scheipl, 2017).

Focusing on shape analysis of sparsely/irregularly curves combining a) and b), we consider the full Procrustes mean concept particularly attractive due to its robustness known from landmark shape analysis and due to its direct connection to the covariance structure of the data, which allows relying on a core estimation strategy in sparse/irregular FDA: following Yao et al. (2005), covariance smoothing has become a major tool for sparse/irregular FDA, allowing to reconstruct the functional covariance structure based on sparse evaluations. Cederbaum et al. (2018); Reiss & Xu (2020) discuss (symmetric) tensor-product spline smoothing for this purpose, considering univariate functional data. Happ & Greven (2018) generalize univariate approaches to conduct functional principal component analysis also for multivariate sparse/irregular data.

In the following, we first discuss complex stochastic processes as random elements of Hilbert spaces, illustrating their convenience for rotation-invariant bivariate FDA and propose Hermitian tensor-product smoothing for complex functional principle component analysis as our first contribution. This lays the groundwork for the second part and second contribution of the paper, where we introduce the notion of elastic (and inelastic) full Procrustes mean shapes of plane curves based on the SRV-framework. We show conditions under which sparsely/irregularly observing SRVs of curves (i.e., curve derivatives) is feasible and propose estimation of their full Procrustes means via Hermitian covariance smoothing. Finally, we present an elastic full Procrustes analysis of tongue outlines observed from participants of a phonetic study and validate the proposed approach in two simulation scenarios. Additional proofs not included in the main manuscript are given in the appendix. A ready to use implementation is offered in the R-package `elastes` (github.com/mpff/elastes).

2. HERMITIAN COVARIANCE SMOOTHING

2.1. Complex processes and rotation invariance

Although functional data analysis traditionally focuses on Hilbert spaces over \mathbb{R} (compare, e.g., Hsing & Eubank, 2015), underlying functional analytic statements cover Hilbert spaces over \mathbb{C} as well (e.g., Rynne & Youngson, 2007). This lets us formulate principal component analysis for complex-valued functional data and underlying concepts in analogy to the real case in the following. Subsequently, we present two results on the relation of complex and bivariate real functional data and its convenience under rotation invariance that will be key in our estimation approach. This adds a new perspective also to previous literature on complex stochastic processes (Neeser & Massey, 1993). Here, the real plane \mathbb{R}^2 is identified with the complex numbers \mathbb{C} via the canonical vector space isomorphism $\kappa : \mathbb{C} \rightarrow \mathbb{R}^2$, $z \mapsto \mathbf{z} = (\Re(z), \Im(z))^\top$ mapping $z \in \mathbb{C}$ to its real part $\Re(z)$ and imaginary part $\Im(z)$. By z^\dagger we denote the complex conjugate $\Re(z) - \mathbf{i}\Im(z)$ of $z \in \mathbb{C}$, with $\mathbf{i}^2 = -1$, or more generally the Hermitian adjoint (conjugate transpose) for complex matrices or operators. Rotation of $\mathbf{z} \in \mathbb{R}^2$ by $\omega \in \mathbb{R}$ radians simplifies to scalar multiplication $\exp(\mathbf{i}\omega)z \in \mathbb{C}$.

Let Y be a complex-valued stochastic process with realizations $y : \mathcal{T} \rightarrow \mathbb{C}$ in $\mathbb{L}^2(\mathcal{T}, \mathbb{C})$, where \mathcal{T} is a compact metric space with finite measure ν . Here, $\mathcal{T} = [0, 1]$ is typically the unit interval with ν the Lebesgue measure, and $t \in \mathcal{T}$ is referred to as ‘‘time’’. The complex, separable Hilbert space $\mathbb{L}^2(\mathcal{T}, \mathbb{C})$ of square-integrable complex-valued functions is equipped with the inner product $\langle x, y \rangle = \int x^\dagger(t)y(t) d\nu(t)$ for $x, y \in \mathbb{L}^2(\mathcal{T}, \mathbb{C})$ and the corresponding norm $\|\cdot\|$.

DEFINITION 1. *i) Y is called random element in a real or complex Hilbert space \mathbb{H} if $\langle x, Y \rangle$ is measurable for all $x \in \mathbb{H}$ and the distribution of Y is uniquely determined by the (marginal) distributions of $\langle x, Y \rangle$ over $x \in \mathbb{H}$.*

ii) The mean $\mu \in \mathbb{H}$ and covariance operator $\Sigma : \mathbb{H} \rightarrow \mathbb{H}$ of a random element Y are defined via $\langle \mu, x \rangle = \mathbb{E}(\langle Y, x \rangle)$ and $\langle \Sigma(x), y \rangle = \mathbb{E}(\langle x, Y - \mu \rangle \langle Y - \mu, y \rangle)$ for all $x, y \in \mathbb{H}$.

In the following, we assume Y is a random element of $\mathbb{L}^2(\mathcal{T}, \mathbb{C})$. Being self-adjoint and compact, its covariance operator Σ admits a representation $\Sigma(f) = \sum_{k \geq 1} \lambda_k \langle e_k, f \rangle e_k$ via countably many eigenfunctions $e_1, e_2, \dots \in \mathbb{L}^2(\mathcal{T}, \mathbb{C})$, $\Sigma(e_k) = \lambda_k e_k$, with real eigenvalues $\lambda_1 \geq \lambda_2 \geq \dots \geq 0$ of Σ (see Appendix). The $\{e_k\}_k$ form an orthonormal basis of the Hilbert subspace formed by the closure of the image of Σ . The random element can be represented as $Y = \mu + \sum_{k \geq 1} \langle e_k, Y \rangle e_k$ with probability one. The scores $Z_k = \langle e_k, Y \rangle$, $k \geq 1$, are complex random variables with mean zero and covariance $\mathbb{E}(\langle Y, e_k \rangle \langle e_{k'}, Y \rangle) = \lambda_k \mathbf{1}_{\{k=k'\}}(k)$, where $\mathbf{1}_S(t) = 1$ if $t \in S$ and 0 else for a set S .

Y is canonically identified with the bivariate real process $\mathbf{Y} = \kappa(Y) = (\Re(Y), \Im(Y))^\top$, random element in the Hilbert space $\mathbb{L}^2(\mathcal{T}, \mathbb{R}^2)$ with the inner product of $\mathbf{x} = \kappa(x)$, $\mathbf{y} = \kappa(y)$, $x, y \in \mathbb{L}^2(\mathcal{T}, \mathbb{C})$, defined by $\langle \mathbf{x}, \mathbf{y} \rangle = \int \Re(x(t)) \Re(y(t)) d\nu(t) + \int \Im(x(t)) \Im(y(t)) d\nu(t) = \Re(\langle x, y \rangle)$.

THEOREM 1. *Define the pseudo-covariance operator Ω of Y with mean μ by $\langle \Omega(x), y \rangle = \mathbb{E}(\langle Y - \mu, x \rangle \langle Y - \mu, y \rangle)$ for all $x, y \in \mathbb{L}^2(\mathcal{T}, \mathbb{C})$, and let Σ denote the covariance operator of $\mathbf{Y} = \kappa(Y)$. Then the covariance and pseudo-covariance operators Σ and Ω of Y together determine Σ via*

$$\kappa^{-1} \circ \Sigma \circ \kappa = (\Sigma + \Omega)/2.$$

Proof. For $x, y \in \mathbb{L}(\mathcal{T}, \mathbb{C})$, $\Re(\langle \Sigma(x) + \Omega(x), y \rangle) = \Re(\mathbb{E}(\langle x, Y \rangle \langle Y, y \rangle + \langle Y, x \rangle \langle Y, y \rangle)) = \Re(\mathbb{E}(2 \Re(\langle Y, x \rangle \langle Y, y \rangle))) = 2 \mathbb{E}(\Re(\langle Y, x \rangle) \Re(\langle Y, y \rangle)) = 2 \langle \Sigma(\kappa(x)), \kappa(y) \rangle$ when assuming $\mu = 0$ for without loss of generality. \square

Aiming at shape analysis, we are particularly interested in rotation-invariant distributions $\mathfrak{L}(\mathbf{Y})$ of $\mathbf{Y} = \kappa(Y)$, i.e., with $\mathfrak{L}(Y) = \mathfrak{L}(\exp(\mathbf{i}\omega)Y)$ for all $\omega \in \mathbb{R}$. In this case, $\mathfrak{L}(Y)$ is typically referred to as ‘proper’, ‘circular’ or ‘complex symmetric’ (Neuser & Massey, 1993; Picinbono, 1996; Kent, 1994) and the simplification in the complex approach becomes evident:

THEOREM 2. *A stochastic process Y with covariance operator Σ with eigenbasis $\{e_k\}_k$ and corresponding eigenvalues $\{\lambda_k\}_k$ follows a complex symmetric distribution if and only if all scores $Z_k = \langle e_k, Y \rangle$ with $\lambda_k > 0$ do and the mean of Y is $\mu = 0$. In this case,*

- i) *the pseudo-covariance Ω of Y vanishes, i.e. $\Omega(y) = 0$ for all $y \in \mathbb{L}^2(\mathcal{T}, \mathbb{C})$, and the covariance operator Σ of the bivariate process $\mathbf{Y} = \kappa(Y)$ is completely determined by Σ ;*
- ii) *the pairs $\mathbf{e}_k = \kappa(2^{-1/2}e_k)$, $\mathbf{e}_{-k} = \kappa(\mathbf{i}2^{-1/2}e_k) \in \mathbb{L}^2(\mathcal{T}, \mathbb{R}^2)$ yield an eigen decomposition $\Sigma(\mathbf{f}) = \sum_{k \neq 0} \lambda_k \langle \mathbf{e}_k, \mathbf{f} \rangle \mathbf{e}_k$ of Σ . With probability one, $\mathbf{Y} = \sum_{k \neq 0} \mathbf{e}_k \mathbf{Z}_k$ with uncorrelated real scores \mathbf{Z}_k with mean zero, variance $\text{var}(\mathbf{Z}_k) = \lambda_k$ and $\kappa(\mathbf{Z}_k) = (\mathbf{Z}_k, \mathbf{Z}_{-k})^\top$.*

Proof. From complex symmetry of $\mathfrak{L}(Y)$ it follows that $\mathfrak{L}(\exp(\mathbf{i}\omega)Z_k) = \mathfrak{L}(\langle e_k, \exp(\mathbf{i}\omega)Y \rangle) = \mathfrak{L}(Z_k)$, $\langle \mu, f \rangle = \mathbb{E}(\langle Y, f \rangle) = \mathbb{E}[\langle -Y, f \rangle] = 0$, and $\langle \Omega(e), f \rangle = \mathbb{E}(\langle Y, e \rangle \langle Y, f \rangle) = \mathbb{E}(-\langle Y, e \rangle \langle Y, f \rangle) = 0$ for all ω, k, e, f , which yields the first direction of the characterization via scores and, together with Lemma 1, statement i). ii) follows from Lemma 1, statement i) and the fact that if Z_k is complex symmetric, $\kappa(Z_k)$ has uncorrelated components with equal variance. Since $\exp(\mathbf{i}\omega)Y = \sum_{k \geq 1} \exp(\mathbf{i}\omega)Z_k e_k$ almost surely if $\mu = 0$, the second direction of the characterization via scores follows. \square

While rotation invariance of $\mathfrak{L}(\mathbf{Y})$ leads to even multiplicities in the eigenvalues of the bivariate covariance operator Σ , the complex eigen decomposition is per se rotation invariant. Here, rotation invariance of $\mathfrak{L}(\mathbf{Y})$ instead translates to complex symmetry of the distribution of the scores Z_k .

Mean and covariance structure of Y can also be approached from the point-wise mean $\mu^*(t) = \mathbb{E}(Y(t))$ and Hermitian covariance surface $C(s, t) = \mathbb{E}(Y^\dagger(s)Y(t)) = C(t, s)^\dagger$. Under complex symmetry, we obtain again $\mu^*(t) = 0$, while the auto-covariances $\mathbb{E}(\Re(Y(s))\Re(Y(t))) = \mathbb{E}(\Im(Y(s))\Im(Y(t))) = \Re(C(s, t))$ and cross-covariances $\mathbb{E}(\Re(Y(s))\Im(Y(t))) = -\mathbb{E}(\Im(Y(s))\Re(Y(t))) = \Im(C(s, t))$ of the bivariate \mathbf{Y} are completely determined by $C(s, t)$, as shown in the Appendix. The integral operator $\Sigma^*(f)(t) = \int C(s, t)f(s) d\nu(s)$ on $\mathbb{L}^2(\mathcal{T}, \mathbb{C})$ induced by the covariance surface again constitutes a compact and self-adjoint operator and admits, as such, an eigen decomposition. In fact, under standard assumptions, such as continuity of $\mu^*(t)$ and $C(s, t)$, Fubini allows switching integrals such that the point-wise mean $\mu^* = \mu$ coincides with the mean element and the operator $\Sigma^* = \Sigma$ with the covariance operator. In this case, the eigen decomposition of Σ also yields a decomposition

$$C(s, t) = \sum_{k \geq 1} \lambda_k e_k^\dagger(s) e_k(t)$$

of the covariance surface.

2.2. Covariance estimation via tensor-product smoothing

Based on a densely/regularly sampled collection of realizations $y_1, \dots, y_n : \mathcal{T} \rightarrow \mathbb{C}$ (with equal grids) of a complex symmetric process Y , the covariance surface $C(s, t)$ of Y can be estimated by the empirical covariance surface $\hat{C}_{emp.}(s, t) = \frac{1}{n} \sum_{i=1}^n y_i^\dagger(t) y_i(s)$ for each pair of grid-points s, t . This is, however, not possible in a sparse/irregular setting where only a limited number of evaluations $y_i(t_{i1}) = y_{i1}, \dots, y_i(t_{in_i}) = y_{in_i}$ are available for $i = 1, \dots, n$ such

that, for a given (s, t) -tuple, $\hat{C}_{emp.}(s, t)$ would only be based on few observations if computable at all. Consequently, some kind of smoothing over samples becomes necessary and, following the seminal work of Yao et al. (2005), covariance estimation in the sparse/irregular functional case has widely been approached as a non-/semi-parametrical regression problem. We proceed accordingly in the complex case and model $\mathbb{E}(Y^\dagger(s)Y(t)) = C(s, t)$ with a (smooth) regression estimator $\hat{C}(s, t)$ fitted to response products $y_{ij}^\dagger y_{ij}$ at respective tuples $(t_{ij}, t_{ij}) \in \mathcal{T}^2$, for $j, \bar{j} = 1, \dots, n_i$ and $i = 1, \dots, n$. Here, it is often reasonable to assume that, in fact, only measurements $\tilde{y}_{ij} = y_{ij} + \varepsilon_{ij}$ are observed with $\varepsilon_{ij} = \varepsilon_i(t_{ij})$ uncorrelated measurement errors originating from a white noise error process $\varepsilon(t)$, $t \in \mathcal{T}$. This leads to a combined covariance $\tilde{C}(s, t) = C(s, t) + \tau^2(t) 1_{\{s\}}(t)$ with $\tau^2(t) = \text{var}(\varepsilon(t))$ the variance function of $\varepsilon(t)$. Assuming $C(s, t)$ continuous, $\tau^2(t)$ can be distinguished as a discontinuous ‘‘nugget effect’’ at $s = t$.

Generalizing the approach of Cederbaum et al. (2018) for real covariance surfaces to the complex case, we propose to model $C(s, t)$ using a Hermitian tensor-product smooth

$$C(s, t) \approx \sum_{g=1}^m \sum_{k=1}^m \xi_{gk} f_g(s) f_k(t) = \mathbf{f}^\top(s) \mathbf{\Xi} \mathbf{f}(t) = \text{vec}(\mathbf{\Xi})^\top (\mathbf{f}(t) \otimes \mathbf{f}(s))$$

with real-valued basis functions $f_k : \mathcal{T} \rightarrow \mathbb{R}$, $k = 1, \dots, m$, stacked to a vector $\mathbf{f}(t) = (f_1(t), \dots, f_m(t))^\top$ and a Hermitian coefficient matrix $\mathbf{\Xi} = \{\xi_{kk'}\}_{kk'} = \mathbf{\Xi}^\dagger \in \mathbb{C}^{m \times m}$ ensuring $\hat{C}(s, t)$ is Hermitian as required. Both the symmetry of the real part $\Re(\mathbf{\Xi}) = \Re(\mathbf{\Xi})^\top$ and the anti-symmetry of the imaginary part $\Im(\mathbf{\Xi}) = -\Im(\mathbf{\Xi})^\top$ present linear constraints. As such they can be implemented via suitable basis transforms $\mathbf{D}_\Re(\mathbf{f} \otimes \mathbf{f})(s, t)$ and $\mathbf{D}_\Im(\mathbf{f} \otimes \mathbf{f})(s, t)$ of the tensor-product basis $(\mathbf{f} \otimes \mathbf{f})(s, t) = (f_1(s)\mathbf{f}^\top(t), \dots, f_m(s)\mathbf{f}^\top(t))^\top$ with vec stacking the columns of a matrix to a vector and transformation matrices $\mathbf{D}_\Re \in \mathbb{R}^{(m^2+m)/2 \times m^2}$ and $\mathbf{D}_\Im \in \mathbb{R}^{(m^2-m)/2 \times m^2}$ for the symmetric and anti-symmetric part, respectively. Since $\mathbb{R}^{m \times m}$ is a direct sum of the vector spaces of symmetric and antisymmetric $m \times m$ matrices, \mathbf{D}_\Im can be obtained, e.g., as basis matrix of the null space of \mathbf{D}_\Re . A possible construction of \mathbf{D}_\Re is described by Cederbaum et al. (2018). In addition to the covariance, we also model the error variance $\tau^2(t) \approx \boldsymbol{\xi}_\tau^\top \mathbf{f}_\tau(t)$ expanded in a real function basis $\mathbf{f}_\tau(t)$. Here, it might be convenient to employ the same basis $\mathbf{f}_\tau(t) = \mathbf{f}(t)$ or to assume constant error variance by setting $\mathbf{f}_\tau(t) = 1$ for all t . For $\tau^2(t) = 0$, the measurement error is excluded from the model. The coefficients $\text{vec}(\hat{\mathbf{\Xi}}) = \mathbf{D}_\Re \hat{\boldsymbol{\xi}}_\Re + \mathbf{i} \mathbf{D}_\Im \hat{\boldsymbol{\xi}}_\Im$ of the covariance estimator $\hat{C}(s, t)$ minimize the penalized least-squares criterion

$$\text{PLS}(\mathbf{\Xi}, \boldsymbol{\xi}_\tau) = \sum_{i,j,\bar{j}} \left| \mathbf{f}^\top(t_{ij}) \mathbf{\Xi} \mathbf{f}(t_{ij}) + \boldsymbol{\xi}_\tau^\top \mathbf{f}_\tau(t_{ij}) 1_{\{\bar{j}\}}(j) - y_{ij}^\dagger y_{i\bar{j}} \right|^2 + \text{PEN}(\mathbf{\Xi}, \boldsymbol{\xi}_\tau)$$

with quadratic penalty term PEN and are separately obtained for the real and imaginary part $\text{PLS} = \text{PLS}_\Re + \text{PLS}_\Im$ of the covariance via the well-known linear estimators $\hat{\boldsymbol{\xi}}_\Re \in \mathbb{R}^{(m^2+m)/2}$, $\hat{\boldsymbol{\xi}}_\tau \in \mathbb{R}^{m_\tau}$ minimizing $\text{PLS}_\Re = \sum_{i,j,\bar{j}} (\boldsymbol{\xi}_\Re^\top \mathbf{D}_\Re(\mathbf{f} \otimes \mathbf{f})(t_{ij}, t_{ij}) - \boldsymbol{\xi}_\tau^\top \mathbf{f}(t_{ij}) 1_{\{\bar{j}\}}(j) - \Re(y_{ij}^\dagger y_{i\bar{j}}))^2 + \eta_\Re \boldsymbol{\xi}_\Re^\top \mathbf{D}_\Re \mathbf{P}_\otimes \mathbf{D}_\Re^\top \boldsymbol{\xi}_\Re$ and $\hat{\boldsymbol{\xi}}_\Im \in \mathbb{R}^{(m^2-m)/2}$ minimizing $\text{PLS}_\Im = \sum_{i,j,\bar{j}} (\boldsymbol{\xi}_\Im^\top \mathbf{D}_\Im(\mathbf{f} \otimes \mathbf{f})(t_{ij}, t_{ij}) - \Im(y_{ij}^\dagger y_{i\bar{j}}))^2 + \eta_\Im \boldsymbol{\xi}_\Im^\top \mathbf{D}_\Im \mathbf{P}_\otimes \mathbf{D}_\Im^\top \boldsymbol{\xi}_\Im$. Smoothing parameters $\eta_\Re, \eta_\Im, \eta_\tau > 0$ control the penalty induced by the matrix $\mathbf{P}_\otimes = \mathbf{P} \otimes \mathbf{I}_m + \mathbf{I}_m \otimes \mathbf{P}$ constructed from a suitable penalty matrix $\mathbf{P} \in \mathbb{R}^{m \times m}$ for the basis coefficients of $\mathbf{f}(t)$ and \mathbf{I}_m the $m \times m$ identity matrix. Assuming the error variance not too heterogeneous over t , the matrix \mathbf{P}_τ should typically penalize deviations from the constant. Based on a working normality assumption, η_\Re, η_τ and η_\Im are obtained via restricted maximum likelihood (REML) estimation (Wood, 2017), avoiding computationally intense hyper-parameter tuning. For practical use,

we extended the R package `sparseFLMM` (Cederbaum, 2018) to also offer anti-symmetric tensor-product smooths for the package `mgcv` (Wood, 2017) used for estimation. For asymptotic theory on the used penalized spline estimators, please see Wood et al. (2016).

After estimation, eigenfunctions e_k and eigenvalues λ_k of the covariance operator Σ of Y are estimated by the corresponding eigen decomposition $\hat{C}(s, t) = \sum_{k \geq 1} \hat{\lambda}_k \hat{e}_k^\dagger(s) \hat{e}_k(t)$ of the respective covariance operator $\hat{\Sigma}$. Based on $\hat{\Xi}$ and the Gram matrix $\mathbf{G} = \{\langle f_k, f_{k'} \rangle\}_{k, k'=1}^m$, the right eigenvalues of the matrix $\mathbf{G}^{-1} \hat{\Xi}$ yield the eigenvalues $\hat{\lambda}_k$ of $\hat{\Sigma}$. The corresponding eigenvectors $\hat{\theta}_k$ yield the eigenfunctions $\hat{e}_k(t) = \hat{\theta}_k^\top \mathbf{f}(t)$ of $\hat{\Sigma}$ for $k = 1, \dots, m$. To ensure positive-definiteness, eigenfunctions with $\lambda_k \leq 0$ are omitted from the basis. Nonnegativity of τ^2 is enforced post-hoc by setting negative values to zero.

3. ELASTIC FULL PROCRUSTES ANALYSIS

3.1. Full Procrustes analysis in the square-root-velocity framework

We understand a *parameterized curve* as a function $\beta : [0, 1] \rightarrow \mathbb{C}$, which is assumed absolutely continuous such that the component-wise derivative $\dot{\beta}(t) = \frac{d}{dt} \Re \circ \beta(t) + \mathbf{i} \frac{d}{dt} \Im \circ \beta(t)$ exists almost-everywhere and also the integral $\varphi_\beta(t) = \int_0^t |\dot{\beta}(s)| ds < \infty$ exists for $t \in [0, 1]$. Denoting the set of absolutely continuous functions $[0, 1] \rightarrow \mathbb{C}$ by $\mathcal{AC}([0, 1], \mathbb{C})$, we further assume $\beta \in \mathcal{AC}^*([0, 1], \mathbb{C}) = \mathcal{AC}([0, 1], \mathbb{C}) \setminus \{t \mapsto z : z \in \mathbb{C}\}$ excluding constant functions as degenerate curves. Then β has positive length $L(\beta) = \varphi_\beta(1) > 0$, and a constant-speed parameterization $\alpha = \beta \circ \varphi_\beta^{-1}$ always exists, when taking the generalized inverse $\varphi_\beta^{-1}(s) = \inf\{t \in [0, 1] : s L(\beta) \leq \varphi_\beta(t)\}$, $s \in [0, 1]$. Two parameterized curves $\beta_1, \beta_2 \in \mathcal{AC}^*([0, 1], \mathbb{C})$ are said to describe the same curve if they have the same constant-speed parameterization $\alpha_1 = \alpha_2$, which yields an equivalence relation $\beta_1 \approx \beta_2$. An *oriented curve* is then defined as equivalence class with respect to ‘ \approx ’. If the context allows it, we commonly refer to both oriented plane curves and their parameterized curve representatives β simply as ‘‘curve’’. A diffeomorphism $\gamma : [0, 1] \rightarrow [0, 1]$ which is orientation-preserving, i.e., with derivative $\dot{\gamma}(t) > 0$ for $t \in [0, 1]$, is called warping function and the set of such warping functions is denoted by Γ . With obviously $\beta \circ \gamma \approx \beta$, warping can equivalently be used to define equivalence of parameterized curves (see, e.g. Bruveris, 2016, which we also recommend for further details). Abstracting also from the particular coordinate system for \mathbb{C} , the shape of an (oriented) curve with parameterization β is then defined by $[\beta] = \{\tilde{\beta} \in \mathcal{AC}([0, 1], \mathbb{C}) \mid \exists u, v \in \mathbb{C} : u \tilde{\beta} + v \approx \beta\}$, its equivalence class under translation, rotation, re-scaling and warping. This presents our ultimate object of interest. In establishing a metric on the quotient space $\mathfrak{B} = \{[\beta] : \beta \in \mathcal{AC}^*([0, 1], \mathbb{C})\}$, we follow the idea of the full Procrustes distance in landmark shape analysis and define

$$d_\Psi([\beta_1], [\beta_2]) = \inf_{\substack{a \geq 0, v_i \in \mathbb{C}, \\ \omega_i \in \mathbb{R}, \gamma_i \in \Gamma}} \|\Psi(\exp(\mathbf{i}\omega_1) \beta_1 \circ \gamma_1 + v_1) - a \Psi(\exp(\mathbf{i}\omega_2) \beta_2 \circ \gamma_2 + v_2)\| \quad (1)$$

for $\beta_1, \beta_2 \in \mathcal{AC}([0, 1], \mathbb{C})$, with a pre-shape map $\Psi : \mathcal{AC}([0, 1], \mathbb{C}) \rightarrow \mathbb{L}^2([0, 1], \mathbb{C})$, $\beta \mapsto q$ discussed below allowing to base computation on the \mathbb{L}^2 -metric while optimizing over all involved invariances. Acting differently than the other curve-shape preserving transformations (see, e.g., Srivastava & Klassen, 2016, Chap. 3.7), scale invariance is generally accounted for by a normalization constraint $\|\Psi(\beta)\| = \|q\| = 1$ for all β . Fixing $a = 1$ in (1) would yield a partial-Procrustes-type distance instead. Replacing also the norm by the arc length on the \mathbb{L}^2 -sphere would correspond to an intrinsic shape distance. To obtain a proper and sound metric, Ψ has to be carefully chosen. It is well-known that directly applying the \mathbb{L}^2 -metric on the level of parame-

terized curves β is problematic, since in this case the warping action of $\gamma \in \Gamma$ is not by isometries (Srivastava & Klassen, 2016).

We set $\tilde{\Psi}(\beta)$ to the SRV-transformation (Srivastava et al., 2011), representing a curve β by its square-root-velocity (SRV) transform $q : [0, 1] \rightarrow \mathbb{C}$ given by $q(t) = \dot{\beta}(t)/|\dot{\beta}(t)|^{1/2}$ wherever this is defined and $q(t) = 0$ elsewhere. Indeed, q is square-integrable with $\|q\|^2 = \int_0^1 |q(t)|^2 dt = L(\beta)$. Since $\tilde{\Psi}(u\beta \circ \gamma + v)(t) = (u/|u|^{1/2})q \circ \gamma(t)\dot{\gamma}(t)^{1/2}$, warping and rotation act by isometries with $\|\tilde{\Psi}(a \exp(\mathbf{i}\omega)\beta_1 \circ \gamma + v) - \tilde{\Psi}(a \exp(\mathbf{i}\omega)\beta_2 \circ \gamma + v)\| = a^{1/2}\|\tilde{\Psi}(\beta_1) - \tilde{\Psi}(\beta_2)\|$ for any two curves β_1, β_2 and $\gamma \in \Gamma$, $a \geq 0$, $\omega \in \mathbb{R}$, $u, v \in \mathbb{C}$. The \mathbb{L}^2 -metric on the SRV-transforms induces a metric on the space of curves modulo translation (Bruveris, 2016). It is commonly referred to as ‘‘elastic’’ metric due to the isometric action of γ allowing to construct a metric on oriented curves via optimal warping alignment. $\tilde{\Psi}$ is surjective but not injective, with $\tilde{\Psi}^{-1}(\{\tilde{\Psi}(\beta)\}) = \{\beta + v : v \in \mathbb{C}\} \subset [\beta]$. Without loss of generality, we can, thus, set $\tilde{\Psi}^{-1}(q)(t) = \int_0^t \dot{\beta}(s) ds = \int_0^t q(s)|q(s)| ds$ for convenience when discussing shapes.

PROPOSITION 1. *With $\Psi(\beta) = \tilde{\Psi}(\beta/L(\beta)) = \tilde{\Psi}(\beta)/\|\tilde{\Psi}(\beta)\|$ the normalized SRV-transform, d_Ψ defines a metric on \mathfrak{B} , referred to as elastic full Procrustes distance $d_\mathcal{E}$. It takes the form*

$$d_\mathcal{E}^2([\beta_1], [\beta_2]) = \inf_{u \in \mathbb{C}, \gamma \in \Gamma} \|q_1 - u q_2 \circ \gamma \dot{\gamma}^{1/2}\|^2 = 1 - \sup_{\gamma \in \Gamma} |\langle q_1, q_2 \circ \gamma \dot{\gamma}^{1/2} \rangle|^2$$

for $q_i = \Psi(\beta_i)$ unit-norm SRV-transforms of curve shape representatives $\beta_1, \beta_2 \in \mathcal{AC}([0, 1], \mathbb{C})$.

Proof. A proof that $d_\mathcal{C}(\beta_1, \beta_2) = \|\Psi(\beta_1) - \Psi(\beta_2)\|$ presents a metric on the space of oriented curves modulo translation is, e.g., provided by Bruveris (2016). The remainder of the proof is analogous to the landmark case and attached in the Appendix. \square

With a metric at hand, we may proceed by considering random shapes and define the concept of a Fréchet mean induced by the metric (compare, e.g., Huckemann, 2012; Ziezold, 1977). A random element A in a metric space (\mathfrak{A}, d) is a Borel-measurable random variable taking values in \mathfrak{A} . A (population) Fréchet mean or expected element $\mathfrak{m} \in \mathfrak{A}$ is defined as a minimizer of the expected square distance

$$\mathbb{E}(d^2(\mathfrak{m}, A)) = \sigma^2 = \inf_{\mathfrak{a} \in \mathfrak{A}} \mathbb{E}(d^2(\mathfrak{a}, A)).$$

assuming a finite variance $\sigma^2 < \infty$.

DEFINITION 2. *A random (plane curve) shape $[B]$ is a random element in the shape space \mathfrak{B} equipped with the elastic full Procrustes distance $d_\mathcal{E}$. We call a Fréchet mean $[\mu_\mathcal{E}] \in \mathfrak{B}$ of $[B]$, represented by $\mu_\mathcal{E} \in \mathcal{AC}([0, 1], \mathbb{C})$, an elastic full Procrustes mean of the random shape $[B]$.*

As distance computation is carried out on SRV-transforms, it is, however, typically more convenient to consider the mean shape via a distribution $\mathfrak{L}(Q)$ of a random element $Q = \Psi(B)$ in the Hilbert space $\mathbb{L}^2([0, 1], \mathbb{C})$ inducing the shape distribution $\mathfrak{L}([B])$.

PROPOSITION 2. *Consider a random element Q in $\mathbb{L}^2([0, 1], \mathbb{C})$ with $\|Q\| = 1$ almost surely. Then the elastic full Procrustes means $[\mu_\mathcal{E}]$ of the induced random shape $[B] = [\Psi^{-1}(Q)]$ are determined by their SRV-transform $\psi_\mathcal{E} = \Psi(\mu_\mathcal{E})$ fulfilling*

$$\psi_\mathcal{E} \in \operatorname{argmax}_{y: \|y\|=1} \mathbb{E} \left(\sup_{\gamma \in \Gamma} |\langle y, Q \circ \gamma \dot{\gamma}^{1/2} \rangle|^2 \right).$$

Proof. $\min_{[\beta] \in \mathfrak{B}} \mathbb{E}(d_\mathcal{E}^2([\beta], [B])) \stackrel{\text{Lemma 1}}{=} \min_{y: \|y\|=1} \mathbb{E}(1 - \sup_{\gamma \in \Gamma} |\langle y, Q \circ \gamma \dot{\gamma}^{1/2} \rangle|^2) = 1 - \max_{y: \|y\|=1} \mathbb{E}(\sup_{\gamma \in \Gamma} |\langle y, Q \circ \gamma \dot{\gamma}^{1/2} \rangle|^2)$. \square

In contrast to the shape invariances, we have no closed form solution for the optimization over $\gamma \in \Gamma$ available. This makes it convenient to also define an *inelastic* full Procrustes mean

of shapes of plane curves with fixed parameterization. It will present a building block in elastic mean estimation but is also interesting in its own right especially in data scenarios involving natural curve parameterizations.

PROPOSITION 3. *For $\beta \in \mathcal{AC}([0, 1], \mathbb{C})$ define the shape of a parameterized plane curve as $(\beta) = \{u\beta + v : u, v \in \mathbb{C}\}$. Then*

- i) *the inelastic full Procrustes distance $d_{\mathcal{G}}((\beta_1), (\beta_2)) = \inf_{u \in \mathbb{C}} \|q_1 - uq_2\|$ with $\|q_i\| = 1$ for $\Psi(\beta_i) = q_i$, $i = 1, 2$, defines a metric on the shape space $\tilde{\mathfrak{B}} = \{(\beta) : \mathcal{AC}([0, 1], \mathbb{C})\}$ of parameterized plane curves and can be expressed as $d_{\mathcal{G}}^2((\beta_1), (\beta_2)) = 1 - |\langle q_1, q_2 \rangle|^2$;*
- ii) *multiplication by $\langle q_1, q_2 \rangle^\dagger / |\langle q_1, q_2 \rangle| = \operatorname{argmin}_{u: |u|=1} \|q_1 - uq_2\|$ yields rotation alignment of β_2 to β_1 ;*
- iii) *for a complex symmetric random element Q in $\mathbb{L}^2([0, 1], \mathbb{C})$ with covariance operator Σ , let $\mathcal{Y}_1 = \{y : \Sigma(y) = \lambda_1 y\}$ denote the spectrum of the leading eigenvalue λ_1 of Σ . Then, $(\mathcal{Y}_1) = \{(y) : y \in \mathcal{Y}_1\}$ is the set of Fréchet means of the random shape $(B) = (\Psi^{-1}(Q))$ in $\tilde{\mathfrak{B}}$ with respect to $d_{\mathcal{G}}$, which we refer to as inelastic full Procrustes means. In particular, the leading eigenvector $\psi_{\mathcal{G}} = e_1$ of an eigen decomposition of Σ yields an inelastic full Procrustes mean $(\mu_{\mathcal{G}})$ of (B) with SRV-transform $\psi_{\mathcal{G}} = \Psi(\mu_{\mathcal{G}})$. It is unique if λ_1 has multiplicity 1. The variance of (B) is $\sigma_{\mathcal{G}}^2 = \mathbb{E}(d_{\mathcal{G}}^2((\mu_{\mathcal{G}}), (B))) = 1 - \lambda_1$.*

Proof. i) and ii) have been shown as part of the proof of Lemma 1 (cf. the Appendix). Analogous to Lemma 2, $\psi_{\mathcal{G}} \in \operatorname{argmax}_{y: \|y\|=1} \mathbb{E}(|\langle y, Q \rangle|^2)$, and $\mathbb{E}(|\langle y, Q \rangle|^2) = \langle y, \Sigma(y) \rangle = \langle y, \sum_k \lambda_k \langle e_k, y \rangle e_k \rangle = \sum_k \lambda_k |\langle e_k, y \rangle|^2 \leq \lambda_1 \sum_k |\langle e_k, y \rangle|^2 = \lambda_1 \|y\|^2 = \lambda_1$, due to $\lambda_k \leq \lambda_1$ and $\|y\| = 1$, with equality attained by all $y = \frac{x}{\|x\|}$ with $x \in \mathcal{Y}_1$. This also yields $(\mu_{\mathcal{G}})$ and $\sigma_{\mathcal{G}}^2$. \square

Imposing a complex symmetry assumption on a curve sample, this lets us utilize Hermitian covariance smoothing for estimating inelastic full Procrustes means.

3.2. The square-root-velocity representation in a sparse/irregular setting

In practice, the shape of an (oriented) plane curve is observed via a vector $\mathbf{b} = (b_0, \dots, b_{n_0})^\top \in \mathbb{C}^{n_0+1}$ of points, which can be considered evaluations $\beta^*(t_j^*) = b_j$ of some continuous parameterization $\beta^* : [0, 1] \rightarrow \mathbb{C}$ of the curve at arbitrary time points $t_0^* < \dots < t_{n_0}^*$. However, fixing the time grid, the derivatives $\dot{\beta}^*(t_i^*)$ are not observable. Instead, evaluations of an SRV-transform describing the curve can be directly obtained from the finite differences $\Delta_j = b_j - b_{j-1}$, if the curve segments $\beta^* \left((t_{j-1}^*, t_j^*) \right) \subset \mathbb{C}$ between the observed points in \mathbf{b} have no edges or loops:

THEOREM 3 (FEASIBLE SAMPLING). *If β^* is continuous and $\beta^* : (t_{j-1}^*, t_j^*) \rightarrow \mathbb{C}$ is injective and continuously differentiable with $\dot{\beta}^*(t) \neq 0$ for all $t \in (t_{j-1}^*, t_j^*)$, for $j = 1, \dots, n_0$, then for any time points $0 < t_1 < \dots < t_{n_0} < 1$ and speeds $w_1, \dots, w_{n_0} > 0$, there exists a $\gamma \in \Gamma$ such that*

$$q(t_j) = w_j^{1/2} (\beta^*(t_j^*) - \beta^*(t_{j-1}^*)) = w_j^{1/2} \Delta_j \quad (j = 1, \dots, n_0)$$

for the SRV-transform q of $\beta = \beta^* \circ \gamma$.

Proof. A proof based on Jordan's Curve Theorem is provided in the Appendix. \square

We call a sample \mathbf{b} of a curve feasible if the conditions of Lemma 3 hold. This is always fulfilled if there is a $\beta^* \in (\beta)$ such that β^* is continuously differentiable with non-vanishing derivative on all $(0, 1)$ and, in particular, if it describes an embedded one-dimensional differentiable submanifold. However, if the curve has edges, they must be contained in \mathbf{b} , as well as a point inside of each loop.

Selected time points $t_1 < \dots < t_{n_0}$ and speeds $w_1, \dots, w_{n_0} > 0$ implicitly determine the parameterization. In principle, they could be arbitrarily selected, but with regard to mean estimation it is desirable to initialize them in a coherent way. Without any prior knowledge, constant speed parameterization of underlying curves β presents a canonical choice. To approximate this, we borrow from constant speed parameterization $\hat{\beta}$ of the sample polygon with vertices \mathbf{b} , implying a piece-wise constant SRV-transform $\hat{q}(t) = \sum_{j=1}^{n_0} q_j 1_{[s_{j-1}, s_j)}(t)$ with SRVs $q_j = \Delta_j |\Delta_j|^{-1} L^{1/2}(\hat{\beta})$, with $L(\hat{\beta}) = \sum_{j=1}^{n_0} |\Delta_j|$ the length of the polygon. The nodes $s_j = \sum_{l=1}^j |\Delta_l| / L(\hat{\beta})$ indicate the vertices $\hat{\beta}(s_j) = b_j$, $j = 0, \dots, n_0$. In accordance with that, we set $q(t_j) = q_j$ and select time points $t_j = (s_j + s_{j-1})/2$ in the center of the edges, for $j = 1, \dots, n_0$. Depending on the context other choices might be preferable, but we generally expect this choice to imply reasonable starting parameterizations.

3.3. Estimating elastic full Procrustes means via Hermitian covariance smoothing

Consider a collection of sample vectors $\mathbf{b}_i \in \mathbb{C}^{n_i+1}$ of n curves $\beta_i \in \mathcal{AC}([0, 1], \mathbb{C})$, $i = 1, \dots, n$, realizations of a random plane curve shape $[B]$. For scale-invariance, sample polygons are normalized to unit-length. Moreover, the \mathbf{b}_i are assumed feasibly sampled to represent them by evaluations $q_i(t_{ij}) = q_{ij}$ at time points t_{ij} , $j = 1, \dots, n_i$, of the SRV-transform q_i of β_i as described in the previous Subsection 3.2. We model an elastic full Procrustes mean $[\mu]$ of $[B]$ via the SRV-transform ψ of $\mu \in \mathcal{AC}([0, 1], \mathbb{C})$ expanded as $\psi(t) = \sum_{k=1}^m \theta_k f_k(t) = \boldsymbol{\theta}^\top \mathbf{f}(t)$ in a basis $\mathbf{f}(t) = (f_1(t), \dots, f_m(t))^\top$ of functions $f_k \in \mathbb{L}^2([0, 1], \mathbb{R})$, $k = 1, \dots, m$, with complex coefficient vector $\boldsymbol{\theta} = (\theta_1, \dots, \theta_m)^\top \in \mathbb{C}^m$. For the basis, piece-wise linear B-splines of order 1 present an attractive choice, since they have been proven identifiable under warping-invariance (Steyer et al., 2021) while still implying continuity of ψ and a differentiable mean curve μ .

The idea of alternating between a) mean estimation on aligned data and b) alignment of the data to the current mean is used for estimation of landmark full Procrustes means (Dryden & Mardia, 2016, p. 139) and intrinsic elastic mean curve shapes (Srivastava & Klassen, 2016, p. 319). We follow a similar strategy to find an estimator $\hat{\psi}(t) = \hat{\boldsymbol{\theta}}^\top \mathbf{f}(t)$ for ψ but estimate an in-elastic full Procrustes mean in a) and base the estimate on Hermitian covariance smoothing for irregularly/sparsely sampled curves. The covariance estimate is also used for estimating normalization and rotation alignment multipliers, which are not directly computable for sparse curve data. For warping alignment in b), we utilize the approach of Steyer et al. (2021), which has also proven suitable for irregularly/sparsely sampled curves. Involved steps of the algorithm are detailed in the following and a discussion of its empirical performance is given in the next section.

Initialize in iteration $h = 0$ SRV-representations $q_i^{[h]}(t_{ij}^{[h]}) = q_{ij}^{[h]}$ with $q_{ij}^{[0]} = q_{ij}$ and $t_{ij}^{[0]} = t_{ij}$ for all i, j , and repeat the following steps:

- I. **Covariance estimation:** We estimate the covariance surface $C^{[h]}(s, t)$ of a complex symmetric process Q underlying $q_1^{[h]}, \dots, q_n^{[h]}$ with a tensor-product estimator $\hat{C}^{[h]}(s, t) = \mathbf{f}(s)^\top \hat{\boldsymbol{\Xi}}^{[h]} \mathbf{f}(t)$ with coefficient matrix $\hat{\boldsymbol{\Xi}}^{[h]} \in \mathbb{C}^{m \times m}$. While for dense sampling, an estimate can be directly obtained from the covariance of the $\langle q_i^{[h]}, f_k \rangle$ (Appendix), we propose Hermitian covariance smoothing as described in Section 2 for sparse/irregular data. This also yields eigenfunctions $\hat{e}_k^{[h]}$ and eigenvalues $\hat{\lambda}_k^{[h]}$, $k = 1, \dots, m$, of the corresponding covariance operator $\hat{\Sigma}^{[h]}$, as well as an estimate $\hat{\tau}^{2[h]}(t) \geq 0$ of the variance of an white noise zero mean residual process $\varepsilon(t)$ at $t \in [0, 1]$, if measurement uncertainty on observations is assumed.
- II. **Mean estimation:** Set $\hat{\psi}^{[h]}(t) = \hat{e}_1^{[h]}(t) = \hat{\boldsymbol{\theta}}^{[h]\top} \mathbf{f}(t)$ to the leading eigenfunction of $\hat{\Sigma}^{[h]}$ obtained from the leading right eigenvector $\hat{\boldsymbol{\theta}}^{[h]}$ of $\mathbf{G}^{-1} \hat{\boldsymbol{\Xi}}^{[h]}$ with Gramian \mathbf{G} of $\mathbf{f}(t)$. This

yields an inelastic full Procrustes mean estimate $[\hat{\mu}^{[h]}] = [\Psi^{-1}(\hat{\psi}^{[h]})]$ of the curves with the current parameterization (Lemma 3), presenting the current estimate of the elastic full Procrustes mean.

- III. **Rotation alignment and re-normalization:** For $u_i^{[h]} = (z_{i1}^{[h]} / |z_{i1}^{[h]}|)^\dagger (L^{[h]}(\beta_i))^{-1/2}$ with $z_{i1}^{[h]} = \langle \hat{e}_k^{[h]}, q_i \rangle$, $u_i^{[h]} q_i^{[h]}$ has norm 1 and is rotation aligned to $\hat{\psi}^{[h]}$. We estimate $u_i^{[h]}$ by $\hat{u}_i^{[h]}$ for $i = 1, \dots, n$ based on the covariance estimation by plugging in conditional expectations $\hat{z}_{ik}^{[h]} = \mathbb{E}(\langle \hat{e}_k^{[h]}, Q \rangle \mid Q(t_j) + \varepsilon(t_j) = q_{ij}^{[h]}, j = 1, \dots, n_i)$ and $\hat{L}^{[h]}(\beta_i) = \mathbb{E}(\|Q\|^2 \mid Q(t_j) + \varepsilon(t_j) = Q_{ij}^{[h]}, j = 1, \dots, n_i)$ under a working normality assumption, an estimation approach in the spirit of Yao et al. (2005). Expressions can be found in the Appendix.
- IV. **Warping alignment:** Based on its rotation aligned SRV evaluations, the i th curve is (approximately) warping aligned to $\mu^{[h]}$ using the approach of Steyer et al. (2021), where SRV-transforms are approximated as piece-wise constant functions $\hat{q}_i^{[h]}(t) \approx q_i^{[h]}(t)$ to find the infimum of $\|\mu^{[h]} - \hat{q}_i^{[h]} \circ \gamma \dot{\gamma}^{1/2}\|$ over $\gamma \in \Gamma$. This yields new parameterization time-points $t_{ij}^{[h+1]}$, $j = 1, \dots, n_i$, and corresponding SRVs $q_{ij}^{[h+1]} = w_{ij}^{[h]} \hat{u}_i^{[h]} q_{ij}^{[h]}$, with suitable $w_{ij}^{[h]} > 0$, passed forward to proceed with the next iteration at Step I. Details can be found in the Appendix.

Stop the algorithm when $\|\hat{\psi}^{[h]} - \hat{\psi}^{[h-1]}\|$ below a specified threshold in Step II. An additional execution of Step III then yields rotation aligned samples of approximately unit-length curves and current time points.

4. ADEQUACY AND ROBUSTNESS OF ELASTIC FULL PROCRUSTES MEAN ESTIMATION IN REALISTIC CURVE SHAPE DATA

Familiar everyday shapes offer an ideal platform for evaluation of shape mean estimation, allowing for intuitive and visual assessment of results. We introduce two different such datasets for investigating the performance of elastic full Procrustes mean shape estimation and comparing it to other mean concepts: 1. `digit3.dat` from Dryden & Mardia (2016) comprising a total of 30 handwritten digits “3” sampled at 13 landmarks each; and 2. irregularly sampled spirals $\beta(t) = t \exp(13it)$, $t \in [0, 1]$, with random $n_i \in \{17, \dots, 22\}$ sampling points per spiral or with $n_i \in \{4, \dots, 7\}$ in a very sparse setting, additionally provided with small measurement errors and random rotation, translation and scaling.

Based on `digit3.dat`, we compare our elastic full Procrustes mean estimator $\hat{\mu}_E$ with its inelastic analog $\hat{\mu}_G$ and with an elastic curve mean estimator $\hat{\mu}_C$ taking shape invariances not into account (fitted with R package `elasdics`). Moreover, we investigate fitting performance of $\hat{\mu}_E$ for $n = 4, 10, 30$ observed digits in a simulation. All estimators are fitted using piece-wise constant and piece-wise linear B-splines with 13 equally spaced knots on SRV-level applying 2nd order difference penalties in the covariance estimation for $\hat{\mu}_E$ and $\hat{\mu}_G$ and no penalty for $\hat{\mu}_C$. Figure 1 shows the estimates fitted on the first $n = 4$ digits in the dataset. Without warping alignment, $\hat{\mu}_G$ does not capture the pronounced central nose in the digit “3” as distinctly as $\hat{\mu}_E$. The difference is somewhat smaller when fitting on all $n = 30$ digits (not shown), yet only marginally. Since the data is roughly rotation and scaling aligned, $\hat{\mu}_C$ is very close to $\hat{\mu}_E$ when fitting on all digits. When fitting only on the first $n = 4$ digits in the data, however, $\hat{\mu}_C$ substantially deviates, in particular for the smooth estimator, as shown in Figure 1 (left). This can presumably be attributed to a) $\hat{\mu}_C$ being more affected by the one outlying “3” (top-left) than $\hat{\mu}_E$, and b) the nose pointing into different directions depending on the handwriting. Overall, deficiencies

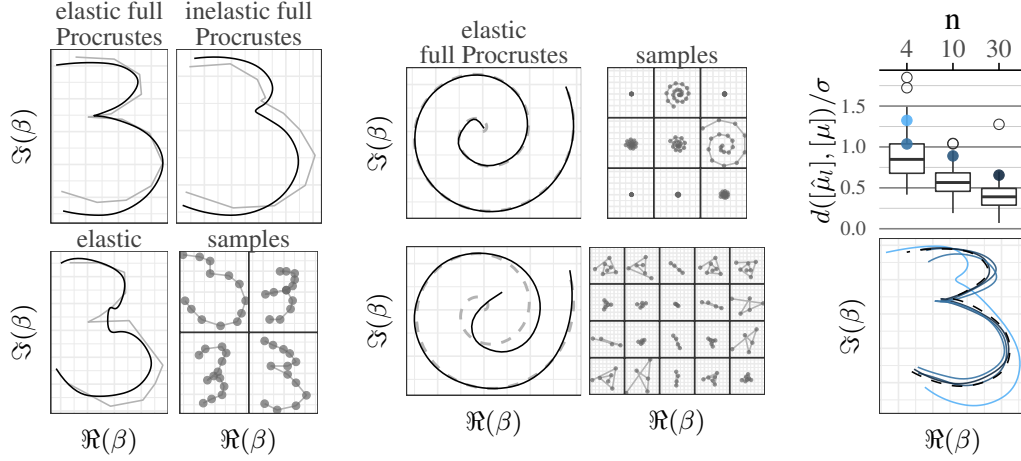


Fig. 1: *Left*: different digit “3” mean curves (*black*: order 1, *grey*: order 0 B-splines on SRV-level) estimated on the first $n = 4$ sample polygons in `digit3.dat` shown in the bottom-right. *Middle*: elastic full Procrustes means estimated on the spiral sample polygons displayed to their right, displayed in front of the original spiral (*grey, dashed line*). *Right*: Simulation results from 101-fold bootstrap samples of different sample sizes on `digit3.dat`. Four bootstrap estimates as examples of cases with relatively high deviations from μ (95% and for $n = 4$ also 75% distance quantiles) are depicted in the bottom and marked in the top panel (*filled dots*). Here, distances to μ are provided relative to the standard deviation σ estimated on the original dataset (as described below in Section 5). Note however, that σ is in some sense an underestimate as it does not include variation induced by irregular/sparse sampling.

in warping and rotation alignment tend to mask features in the curve shapes by averaging over different orientations and parameterizations, similarly to the effect of measurement error in covariates in a regression model. With missing scale alignment, the shape of the estimated mean is mainly driven by the shape of the largest curve(s) in the data.

Good estimation quality is also confirmed in simulations that compare elastic full Procrustes mean estimates $\hat{\mu}_l$, $l = 1, \dots, 101$, estimated on independently drawn bootstrap samples of the digits (with $n = 4, 10, 30$), with the mean μ estimated on the original dataset and taken as true mean. While single mean estimates for as few curves as $n = 4$ might considerably deviate, the majority visually resembles μ well, including $\hat{\mu}_{(0.75)}$ where $\hat{\mu}_{(a)}$ denotes the bootstrap estimator with $d_{(a)}$ the a -quantile of the distances $d_l = d_{\mathcal{E}}([\hat{\mu}_l], [\mu])$, $l = 1, \dots, 101$. Except for two outliers, all estimates with $n = 10$ and $n = 30$ are better than $\hat{\mu}_{(0.75)}$ for $n = 4$ (Figure 1, right).

We illustrate the role of sparsity in shape mean estimation in the spiral data with its varying level of detail over the curve (i.e. varying curvature) and random irregular grids sampled roughly at constant angle distances (Figure 1, middle). Elastic full Procrustes mean estimates are based on piece-wise linear splines on SRV-level with 20 knots and 2nd order penalties in covariance smoothing. With a moderate number of sample points $n_i \in \{17, \dots, 22\}$, the estimate based on $n = 9$ curves regains the original spiral shape close to perfectly. Only the inner end of the spiral with the most curvature shows some deviation. With $n_i \in \{4, \dots, 7\}$ close to the minimum $n_i = 3$ and $n = 20$, the estimator does not capture the higher curvature in the inner part of the spiral but otherwise fits its shape well despite extreme sparsity. In sparse functional data analysis, borrowing of strength across curves allows for consistent estimation of principle components

based on a minimum number of sampling points n_i for each curve under mild conditions (Yao et al., 2005). However, this cannot equally be expected under shape invariances, as indicated by the fact that no shape information remains when curves are observed at $n_i < 3$ points, and in particular when warping-alignment can only be approximated on sparse samples. Still, we observe that bias becomes vanishingly small when the sampling points cover the curve sufficiently well. As this is often the case in real data, elastic full Procrustes mean estimation performs reliably well in practice already for comparably sparse data in our experience.

5. PHONETIC ANALYSIS OF TONGUE SHAPES

The modulation of tongue shape presents an integral part of articulation (Hoole, 1999). Several authors investigate the shape variation in different phonetic tasks by analyzing tongue surface contours during speech production (Stone et al., 2001; Iskarous, 2005; Davidson, 2006) to obtain insights into speech mechanics. They model tongue contour shapes with (penalized) B-splines fitted through points marked on the tongue surface in ultrasound or MRT images of the speaker profile. While different measures to register/superimpose the tongue contour curves are undertaken, shape and warping invariances are not explicitly incorporated into their statistical analysis so far. In particular, reducing tongue shapes to one dimensional curves over an angle as in Davidson (2006) brings the problem that the different functions (due to different tongue shapes for different sounds) extend over different angle domains, which is ignored in the analysis. We suggest elastic full Procrustes analysis to appropriately handle the inherently two-dimensional curves. This approach accounts for the lack of a coordinate system in the ultrasound image, different positioning of ultrasound devices and size differences of speakers (Procrustes analysis) as well as flexibility of the tongue muscle to adjust its shape (elastic analysis). We illustrate it in experimental data kindly provided by Marianne Pouplier: tongue contour shapes are recorded in an experimental setting from six native German speakers ($\mathcal{S} = \{1, \dots, 6\}$) repeating the same set of fictitious words, such as “pada”, “pidi”, “pala” or “pili”. The words implement different combinations of two flanking vowels in $\mathcal{V} = \{a * a, i * i\}$ around a consonant in $\mathcal{C} = \{d, l, n, s\}$. Each combination is repeated multiple times by each of the speakers (1-8 times), observing tongue contour shapes formed at the central time point of consonant articulation (estimated from the acoustic signal). In total, this yields $n = 299$ sample polygons with nodes $\mathbf{b}_i \in \mathbb{C}^{n_i}$, $i = 1, \dots, n$, each sampled at $n_i = 29$ points from the tongue root to the tongue tip. A feature vector $X_i = (v_i, c_i, s_i)^\top \in \mathcal{X} = \mathcal{V} \times \mathcal{C} \times \mathcal{S}$ identifies the word-speaker combination of the i th curve. We investigate the different sources of shape variability (consonants, vowel context, speakers, repetitions) by elastic Full Procrustes analysis on different levels of hierarchy. Let $[\hat{\mu}_{\mathcal{A}}] \in \mathfrak{B}$ denote the elastic full Procrustes mean estimated for all i with $X_i \in \mathcal{A} \subset \mathcal{X}$. Figure 2 depicts the overall shape mean $[\hat{\mu}_{\mathcal{X}}]$, separate means $[\hat{\mu}_{\{(c,v)\} \times \mathcal{S}}]$ for the consonants $c \in \{d, s\}$ in both vowel contexts $v \in \mathcal{V}$, and speaker-word means $[\hat{\mu}_{\{(c,v,s)\}}]$ reflecting individual articulation by speaker $s \in \mathcal{S}$. Not displayed consonants “l” and “n” yield very similar shapes as “d”. Shape means are estimated using linear B-splines on SRV level with 13 equidistant knots and a 2nd order difference penalty for the basis coefficients. Homogeneous measurement error variance is assumed. Fitting the overall mean in this setting takes about 3 minutes on a standard computer.

For quantitative assessment of the hierarchical variation structure, we consider the conditional variances $\sigma_{\mathcal{A}}^2 = \mathbb{E}(d_{\mathcal{E}}^2([B], [\mu_{\mathcal{A}}]) \mid X \in \mathcal{A})$ for the random tuples $([B], X)$ in $\mathfrak{B} \times \mathcal{X}$ with X constrained on a subset $\mathcal{A} \subset \mathcal{X}$, which we estimate by $\hat{\sigma}_{\mathcal{A}}^2 = 1 - \hat{\lambda}_{\mathcal{A},1}(\sum_{k=1}^m \hat{\lambda}_{\mathcal{A},k})^{-1}$ with $\hat{\lambda}_{\mathcal{A},1}, \dots, \hat{\lambda}_{\mathcal{A},m}$ the positive eigenvalues of the covariance operator obtained in the final iter-

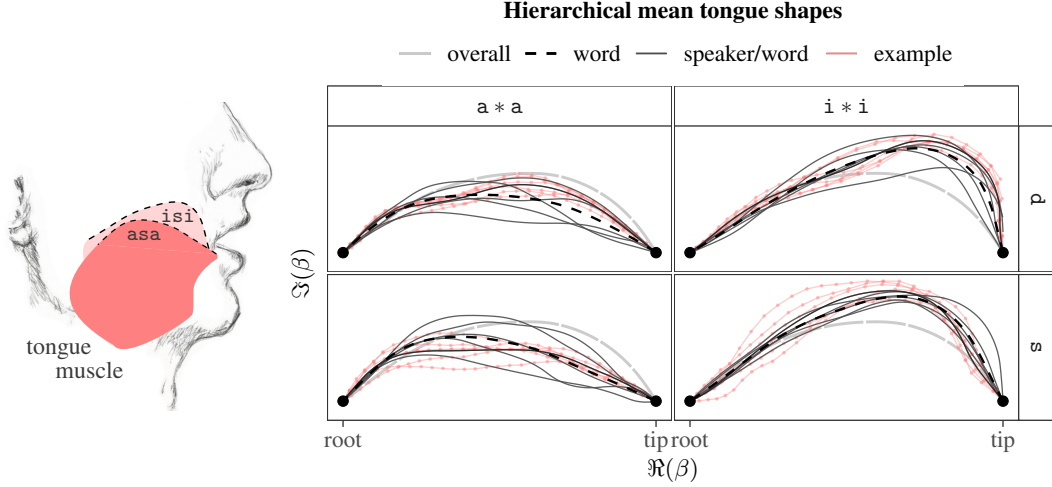


Fig. 2: *Left*: schematic illustrating the tongue muscle modulation when pronouncing “isi” and “asa”. Dashed lines correspond to the respective mean shapes in the right plot. With its multiple and multi-directional fibers, the tongue muscle almost fills the entire oral cavity and can flexibly adjust its shape. In particular, not only tongue tip but also tongue root can move relatively freely. *Right*: elastic full Procrustes mean tongue shape estimates for different levels of aggregation. Each panel shows the overall mean shape in the dataset (*light gray, thick long-dashed line*), the vowel-consonant mean shape (*black, dashed line*), and speaker-wise mean shapes (*dark gray, solid lines*) for each combination. In each panel, original sample polygons (*light red, thin lines, dots at sample points*) are added for the speaker with most intra-speaker variation (which is the same speaker except for “idi”). Tongue shapes are depicted in Bookstein coordinates, i.e. with the tongue roots at $\beta(0) = 0$ and the tongue tips at $\beta(1) = 1$.

ation of estimating $[\mu_{\mathcal{A}}]$. In a dense setting, where observations can be exactly normalized, the estimator $\hat{\sigma}_{\mathcal{A}}^2 = 1 - \hat{\lambda}_{\mathcal{A},1}$ can be used directly, since when $\|Q\| = 1$ almost surely also $\mathbb{E}(\|Q\|^2) = \sum_{k \geq 1} \lambda_k = 1$. In a sparse setting, however, dividing by $\sum_{k=1}^m \hat{\lambda}_{\mathcal{A},k}$ in $\hat{\sigma}_{\mathcal{A}}^2$ ensures non-negative variance estimates.

In analogy to standard analysis of variance, we define the coefficient of determination for \mathcal{A}_1 in some decomposition $\mathcal{A}_1 \times \mathcal{A}_2 = \mathcal{X}$ as $R_{\mathcal{A}_1}^2 = 1 - (|\mathcal{X}| \hat{\sigma}_{\mathcal{X}}^2)^{-1} |\mathcal{A}_2| \sum_{a \in \mathcal{A}_1} \hat{\sigma}_{\{a\} \times \mathcal{A}_2}^2$ reflecting the variance reduction achieved by conditioning on the features in \mathcal{A}_1 . Inspecting these measures underpins the visual impression from Figure 2: although the tongue movement is induced by consonant pronunciation, the vowel context appears more dispositive for the tongue shape during articulation explaining more than half of the total variation ($R_{\mathcal{V}}^2 = 0.68$, $R_{\mathcal{C}}^2 = 0.11$), which increases only to $R_{\mathcal{V} \times \mathcal{C}}^2 = 0.73$ when also distinguishing consonants. Comparing the different vowel contexts, we observe nearly double variation for a * a than for i * i with $\hat{\sigma}_{\{a*a\} \times \mathcal{C} \times \mathcal{S}}^2 / \hat{\sigma}_{\{i*i\} \times \mathcal{C} \times \mathcal{S}}^2 = 1.95$, which might potentially relate to different pronunciations of “a” in German dialects. When considering single word articulation of a speaker ($R_{\mathcal{V} \times \mathcal{C} \times \mathcal{S}}^2 = 0.93$) about 7 percent of the variation remain as residual variance, indicating that, while there is still non-negligible intra speaker variation, the inter speaker variance is considerably higher.

Recorded via ultrasound images, the shape of tongue surface contours modulo the respective invariances presents a natural object of analysis. Yet, if suitable reference landmarks allow, the information on positioning, size, orientation and warping of the curve could also be separately investigated.

6. DISCUSSION

While we find good performance of the proposed elastic full Procrustes mean estimator in realistic irregular/sparse curve data, future work should focus on theoretical assessment of estimation quality as well as inference. In particular, evaluation of the bias introduced by sub-optimal alignment of curves based on single discrete measurements would be of interest, as well as characterization of suitable sampling schemes where the bias is empirically negligible, which often appears to be the case in practice. Offering an analytic solution, inelastic full Procrustes analysis can also serve as a good starting point for estimating other types of shape means of plane curves. In addition, the estimated covariance structure may support estimation in sparse/irregular data scenarios, e.g. where scalar products are involved.

ACKNOWLEDGEMENT

We sincerely thank Marianne Pouplier and Philip Hoole for providing their carefully recorded phonetic tongue shape data and Paula Giesler and Sophia Schaffer for their help in understanding and visualizing its anatomical background. We gratefully acknowledge funding by grant GR 3793/3-1 from the German research foundation (DFG).

APPENDIX 1: HERMITIAN COVARIANCE SMOOTHING

Complex processes and rotation invariance

In the following, we detail prerequisites on linear operators. Subsequently, Proposition A2 substantiates the relation of complex and real covariance surface(s) indicated in the main manuscript.

We widely follow Hsing & Eubank (2015) in their introduction of functional data fundamentals, but re-state required statements underlying Section 2.1 for the complex case, since they nominally focus on real Hilbert spaces. Moreover, we give a Bochner integral free definition of mean elements and covariance operators to avoid introduction of additional notions.

Let \mathbb{H} denote a Hilbert space over \mathbb{C} or \mathbb{R} .

THEOREM A1. *Let Ω be a compact self-adjoint operator on \mathbb{H} . Then there exists a sequence of countably many real eigenvalues $\lambda_1, \lambda_2, \dots \in \mathbb{R}$ of Ω with corresponding orthogonal eigenvectors $e_1, e_2, \dots \in \mathbb{H}$ and $\lambda_1 \geq \lambda_2 \geq \dots$ such that $\{e_k\}_k$ (called eigenbasis of Ω) is an orthonormal basis of the closure $\overline{\Omega(\mathbb{H})}$ of the image of Ω and for every $x \in \mathbb{H}$*

$$\Omega(x) = \sum_{k \geq 1} \lambda_k \langle e_k, x \rangle e_k.$$

Proof. Compare Rynne & Youngson (2007), Chapter 7.3. □

DEFINITION A1. *Let Y be a random element in \mathbb{H} with $\mathbb{E}(\|Y\|^2) < \infty$. Then*

- i) the mean element $\mu \in \mathbb{H}$ of Y is defined by $\langle f, \mu \rangle = \mathbb{E}(\langle f, Y \rangle)$ for all $f \in \mathbb{H}$.*
- ii) the covariance operator $\Sigma : \mathbb{H} \rightarrow \mathbb{H}$ of Y is defined by $\langle \Sigma(e), f \rangle = \mathbb{E}(\langle Y - \mu, f \rangle \langle e, Y - \mu \rangle)$ for all $e, f \in \mathbb{H}$.*

PROPOSITION A1. *Consider μ and Σ as above.*

- i) μ and Σ are well-defined.*
- ii) Σ is a nonnegative-definite (thus self-adjoint), trace-class and, hence, also compact linear operator.*

Proof. i) Since $\mathbb{E}(\|Y\|^2) < \infty$, Jensen's inequality yields $\mathbb{E}(\|Y\|) < \infty$, and therefore $\mathbb{E}(\langle f, Y \rangle) < \infty$ and also $\mathbb{E}(\langle Y - \mu, f \rangle \langle e, Y - \mu \rangle) < \infty$ for all $e, f \in \mathbb{H}$. Uniqueness of μ and Σ follow from the Riesz Representation Theorem.

ii) Set $\mu = 0$ without loss of generality. Self-adjointness $\langle \Sigma(e), f \rangle = \mathbb{E}(\langle Y, f \rangle \langle e, Y \rangle) = \langle e, \Sigma(f) \rangle$ and nonnegative-definiteness $\langle \Sigma(e), e \rangle = \mathbb{E}(\langle Y, e \rangle \langle e, Y \rangle) = \mathbb{E}(|\langle e, Y \rangle|^2)$ immediately follow from the definition. Σ is trace-class, since for an orthonormal basis $\{e_k\}_k$ of \mathbb{H} it holds that

$$\sum_k \langle \Sigma(e_k), e_k \rangle = \sum_k \mathbb{E}(|\langle e_k, Y \rangle|^2) = \mathbb{E}(\|Y\|^2) < \infty$$

as assumed in the definition. Trace-class operators are compact. \square

COROLLARY A1. *The covariance operator Σ of Y with $\mathbb{E}(\|Y\|^2) < \infty$ has an eigenbasis as described in Theorem A1.*

Proof. Immediately follows from Theorem A1 and the self-adjointness and compactness of Σ shown in Lemma A1. \square

Relation to bivariate (real) processes

PROPOSITION A2. *Analogous to Σ , the bivariate covariance surface $\mathbf{C}(s, t)$ of $\mathbf{Y} = \kappa(Y)$ in $\mathbb{L}^2([0, 1], \mathbb{R}^2)$ is characterized by the matrix of covariance and cross-covariance surfaces*

$$\mathbf{C}(s, t) = \begin{pmatrix} \mathbb{E}(\Re(Y(s)) \Re(Y(t))) & \mathbb{E}(\Im(Y(s)) \Re(Y(t))) \\ \mathbb{E}(\Re(Y(s)) \Im(Y(t))) & \mathbb{E}(\Im(Y(s)) \Im(Y(t))) \end{pmatrix} = \frac{1}{2} \begin{pmatrix} \Re(C(s, t) + R(s, t)) & \Im(R(s, t) - C(s, t)) \\ \Im(C(s, t) + R(s, t)) & \Re(C(s, t) - R(s, t)) \end{pmatrix}$$

determined by the pseudo-covariance surface $R(s, t) = \mathbb{E}(Y(s)Y(t))$ in addition to the complex covariance surface $C(s, t)$.

Proof.

$$\begin{aligned} C(s, t) + R(s, t) &= \mathbb{E}(Y^\dagger(s)Y(t) + Y(s)Y(t)) = \mathbb{E}((2\Re(Y(s)) + 0)Y(t)) \\ &= 2\mathbb{E}(\underbrace{\Re(Y(s)) \Re(Y(t))}_{\frac{1}{2}\Re(C(s, t) + R(s, t))} + 2\mathbf{i}\mathbb{E}(\underbrace{\Re(Y(s)) \Im(Y(t))}_{\frac{1}{2}\Im(C(s, t) + R(s, t))})) \\ C(s, t) - R(s, t) &= \mathbb{E}(Y^\dagger(s)Y(t) - Y(s)Y(t)) = \mathbb{E}((0 - 2\mathbf{i}\Im(Y(s)))Y(t)) \\ &= -2\mathbf{i}\mathbb{E}(\underbrace{\Im(Y(s)) \Re(Y(t))}_{\frac{1}{2}\Im(R(s, t) - C(s, t))} + 2\mathbb{E}(\underbrace{\Im(Y(s)) \Im(Y(t))}_{\frac{1}{2}\Re(C(s, t) - R(s, t))})) \end{aligned}$$

which shows the desired form. \square

APPENDIX 2: ELASTIC FULL PROCRUSTES ANALYSIS

Full Procrustes analysis in the square-root-velocity framework

In the following, we start by proving Proposition 3 i) and use it to show Proposition 1 subsequently.

Proof Proposition 3. i) $d_{\mathcal{G}}$ defines a metric on \mathfrak{B} :

$$\begin{aligned} d_{\mathcal{G}}^2((\beta_1), (\beta_2)) &= \inf_{u \in \mathbb{C}} \|q_1 - u q_2\|^2 = \inf_{u \in \mathbb{C}} \left[1 - \underbrace{u}_{=r_1 \exp(\mathbf{i}\omega_1)} \underbrace{\langle q_1, q_2 \rangle}_{=r_2 \exp(\mathbf{i}\omega_2)} - u^\dagger \langle q_2, q_1 \rangle + |u|^2 \right] \\ &= \inf_{r_1 > 0, \omega_1 \in \mathbb{R}} \left[1 - r_1 r_2 \exp(\mathbf{i}(\omega_1 + \omega_2)) - r_1 r_2 \exp(-\mathbf{i}(\omega_1 + \omega_2)) + r_1^2 \right] \\ &= \inf_{r_1 > 0, \omega_1 \in \mathbb{R}} \left[1 - 2r_1 r_2 \cos(\omega_1 + \omega_2) + r_1^2 \right] \stackrel{\omega_1 = -\omega_2}{=} \inf_{r_1 > 0} \left[1 - 2r_1 r_2 + r_1^2 \right] \\ &= \inf_{r_1 > 0} \left[1 - r_2^2 + (r_1 - r_2)^2 \right] \stackrel{r_1 = r_2}{=} 1 - |\langle q_1, q_2 \rangle|^2 = \|q_1 - \langle q_2, q_1 \rangle q_2\|^2 \quad (\text{B1}) \end{aligned}$$

Clearly, $d_{\mathcal{G}}$ is well-defined (i.e., does not depend on the choice of $\beta_i \in (\beta_i)$), symmetric, positive. It is zero if and only if $|\langle q_2, q_1 \rangle| = 1$ and, hence, $(\beta_1) = (\int_0^t q_1(s) |q_1(s)| ds) =$

$(\langle q_2, q_1 \rangle \int_0^t q_2(s) |q_2(s)| ds) = (\beta_2)$. To show the triangle inequality let $(\beta_3) \in \tilde{\mathfrak{B}}$ with $q_3 = \Psi(\beta_3)$ and $v^* = \langle q_2, q_1 \rangle$. Then $d_{\mathcal{G}}((\beta_1), (\beta_3)) = \inf_{u \in \mathbb{C}} \|q_1 - u q_3\| \stackrel{\mathbb{L}^2}{\leq} \stackrel{\text{tr. ineq.}}{\leq}$

$$\underbrace{\|q_1 - v^* q_2\|}_{\stackrel{(B1)}{=} \inf_{v \in \mathbb{C}} \|q_1 - v q_2\|} + \underbrace{\inf_{u \in \mathbb{C}} \|v^* q_2 - u q_3\|}_{= |v^*| \inf_{u \in \mathbb{C}} \|q_2 - u q_3\|} \stackrel{|v^*| \leq 1}{\leq} d_{\mathcal{G}}((\beta_1), (\beta_2)) + d_{\mathcal{G}}((\beta_2), (\beta_3)). \quad \square$$

Proof Proposition 1. $d_{\mathcal{E}}$ defines a metric on \mathfrak{B} and allows for the expression provided in the Lemma:

$$\begin{aligned} d_{\mathcal{E}}^2([\beta_1], [\beta_2]) &= \inf_{a \geq 0, v_i \in \mathbb{C}, \omega_i \in \mathbb{R}, \gamma_i \in \Gamma, i=1,2} \left\| \exp(\mathbf{i}\omega_1) q_1 \circ \gamma_1 \dot{\gamma}_1^{1/2} - a \exp(\mathbf{i}\omega_2) q_2 \circ \gamma_2 \dot{\gamma}_2^{1/2} \right\|^2 \\ &\stackrel{(*)}{=} \inf_{u \in \mathbb{C}, \gamma \in \Gamma} \|q_1 - u q_2 \circ \gamma \dot{\gamma}^{1/2}\|^2 \stackrel{(**)}{=} 1 - \sup_{\gamma \in \Gamma} |\langle q_1, q_2 \circ \gamma \dot{\gamma}^{1/2} \rangle|^2 \end{aligned}$$

where $(*)$ follows from isometry of rotation and warping action setting $u = a \exp(\mathbf{i}(\omega_2 - \omega_1))$, $\gamma = \gamma_2 \circ \gamma_1^{-1}$; and $(**)$ is analogous to the proof of Proposition 3.

As Γ acts on \mathfrak{B} by isometries, $\inf_{u \in \mathbb{C}, \gamma \in \Gamma} \|q_1 - u q_2 \circ \gamma \dot{\gamma}^{1/2}\| = \inf_{\gamma \in \Gamma} d_{\mathcal{G}}((\beta_1), (\beta_2))$ is a semi-metric. To see that it is also positive-definite, assume $d_{\mathcal{E}}([\beta_1], [\beta_2]) = 0$. Consider any minimizing sequence $\{u_l\}_l$ with $0 = d_{\mathcal{E}}([\beta_1], [\beta_2]) = \inf_{\gamma \in \Gamma} \lim_{l \rightarrow \infty} \|q_1 - u_l q_2 \circ \gamma \dot{\gamma}^{1/2}\|$. Then, $\{u_l\}_l$ is bounded, since $|u_l| \|q_2\| = \inf_{\gamma \in \Gamma} |u_l| \|q_2 \circ \gamma \dot{\gamma}^{1/2}\| = \inf_{\gamma \in \Gamma} \|u_l q_2 \circ \gamma \dot{\gamma}^{1/2}\| \leq \inf_{\gamma \in \Gamma} \|u_l q_2 \circ \gamma \dot{\gamma}^{1/2} - q_1\| + \|q_1\| = \|q_1\|$ and $\|q_2\| > 0$ since β_1 is assumed non-constant. Hence, there is a convergent subsequence $\lim_{h \rightarrow \infty} u_{l_h} = u$, and $0 = \inf_{\gamma \in \Gamma} \lim_{h \rightarrow \infty} \|q_1 - u_{l_h} q_2 \circ \gamma \dot{\gamma}^{1/2}\| \stackrel{\text{continuity}}{=} \inf_{\gamma \in \Gamma} \|q_1 - u q_2 \circ \gamma \dot{\gamma}^{1/2}\|$ which is known to be a metric on $\mathbf{q}_1 = \kappa(q_1)$, $\mathbf{q}_2 = \kappa(q_2) \in \mathbb{L}^2([0, 1], \mathbb{R}^2)$ (Bruveris, 2016). Hence, also $[\beta_1] = [\beta_2]$ which completes the proof. \square

The square-root-velocity representation in a sparse/irregular setting

THEOREM B1. *Let $\beta : [0, 1] \rightarrow \mathbb{C}$ be continuous, injective, and, for all $t \in (0, 1)$, continuously differentiable with $\dot{\beta}(t) = \frac{d}{dt} \Re \circ \beta(t) + \mathbf{i} \frac{d}{dt} \Im \circ \beta(t) \neq 0$. Then, there exists a $c \in (0, 1)$ such that $\dot{\beta}(c) = \delta(\beta(1) - \beta(0))$ for some $\delta > 0$.*

Proof. Let $\rho = \Re \circ \beta$ and $\zeta = \Im \circ \beta$ denote the real and imaginary part of β . Without loss of generality assume $\beta(0) = 0$ and $\beta(1) = \mathbf{i}$. Choose $0 \leq t_0 < t_1 \leq 1$ with $\rho(t_0) = \rho(t_1) = 0$ such that $\zeta(t) \geq \zeta(t_0)$ for all $t \in [0, 1]$ with $\rho(t) = 0$ and $\zeta(t) \leq \zeta(t_1)$ for all $t \in [t_0, 1]$ with $\rho(t) = 0$. If $\rho(t) = 0$ for all $t \in [t_0, t_1]$ and, hence, $\dot{\beta}(t) = \mathbf{i} \dot{\zeta}(t)$ within (t_0, t_1) , the Mean Value Theorem directly yields existence of the desired $c \in (t_0, t_1)$. We may, thus, assume $\rho(t) \neq 0$ for some $t \in [t_0, t_1]$, say, with $\rho(t) > 0$. Accordingly, a maximizer $c \in [t_0, t_1]$ with $\rho(c) = \max_{t \in [t_0, t_1]} \rho(t) > 0$ lies in (t_0, t_1) and $\dot{\rho}(c) = 0$, since ρ is continuously differentiable. Hence $\dot{\beta}(c) = \mathbf{i} \dot{\zeta}(c) \neq 0$ as β is regular. $t_0 \neq t_1$ and c all exist due to compactness/continuity arguments.

We will now assume $\delta = \dot{\zeta}(c) < 0$ and show that this leads to a contradiction. With some upper/lower bounds $\rho_{\text{sup}} > \rho(c) (> 0)$ and $\zeta_{\text{inf}} < \min_{t \in [0, 1]} \zeta(t)$, we construct the open polygonal curve $\alpha : [c, 1]$ connecting the points $a_1 = \beta(c)$, $a_2 = \rho_{\text{sup}} + \mathbf{i} \zeta_{\text{inf}}$, $a_3 = \mathbf{i} \zeta_{\text{inf}}$ and $a_4 = \beta(t_0) \leq 0$. Then $\beta 1_{[t_0, c]} + \alpha 1_{[c, 1]}$ is a simple closed continuous curve on $[t_0, 1]$, hence splits \mathbb{C} into two connected open components, the interior component $\mathcal{A} \subset \mathbb{C}$ which is bounded and the exterior component $\mathcal{U} = \mathbb{C} \setminus \bar{\mathcal{A}}$ (Jordan curve theorem) where $\bar{\mathcal{A}}$ denotes the closure of \mathcal{A} . The path $\phi : [0, \infty) \rightarrow \mathbb{C}$, $r \mapsto \beta(t_1) + r \mathbf{i}$ does not intersect the boundary $\beta([t_0, c]) \cup \alpha([c, 1]) = \bar{\mathcal{A}} \cap \bar{\mathcal{U}}$ for all $r \geq 0$, since, by construction, $\zeta(t_1) > \Im(a_k)$ for $k = 2, \dots, 4$ and, for all $t \in [t_0, c]$ with $\rho(t) = 0$, $\zeta(t_1) > \zeta(t)$ as $\zeta(t_1) \geq \zeta(t)$, $c < t_1$ and β injective. Thus, ϕ lies entirely in \mathcal{A} or in \mathcal{U} . Since \mathcal{A} is bounded, the path and, in particular, $\phi(0) = \beta(t_1) \in \mathcal{U}$. Due to the construction of α and injectivity of β that do not permit intersection of the boundary (Jordan curve), $\beta(t)$ lies in \mathcal{A} for all $t > c$ if it lies within \mathcal{A} for some $t > c$. This makes the local behavior at c crucial. Thus, the assumption of $\dot{\zeta}(c) < 0$ entailing $\beta(t) \in \mathcal{A}$ for some $t > 0$ yields, in particular, $\beta(t_1) \in \mathcal{A}$ and, hence, the desired contradiction. \square

COROLLARY B1 (FEASIBLE SAMPLING). *If $\beta^* : [0, 1] \rightarrow \mathbb{C}$ is continuous and $\beta^* : (t_{j-1}^*, t_j^*) \rightarrow \mathbb{C}$ continuously differentiable for $j = 1, \dots, n_0$, $t_0^* < \dots < t_{n_0}^*$ with non-vanishing derivative, then for any*

time points $0 < t_1 < \dots < t_{n_0} < 1$ and speeds $w_1, \dots, w_{n_0} > 0$, there exists a $\gamma \in \Gamma$ such that for the SRV-transform q of $\beta = \beta^* \circ \gamma$, $q(t_j) = w_j^{1/2} (\beta^*(t_j^*) - \beta^*(t_{j-1}^*)) = w_j^{1/2} \Delta_j$ for all $j = 1, \dots, n_0$.

Proof. Since this is a local property, it suffices to consider the case of $n_0 = 1$ and $t_0^* = 0, t_1^* = 1$. By Lemma B1, there exists $c \in (0, 1)$ with $\dot{\beta}(c)^* = a \Delta_1$ for some $a > 0$. Choose $\gamma \in \Gamma$ such that $\gamma(t_1) = c$ and $\dot{\gamma}(t_1) = w_1 a^{-2}$. Then, $q(t_j) = \beta^* \circ \gamma(t_j) \dot{\gamma}(t_j)^{1/2} = a \Delta_1 w_1^{1/2} a^{-1} = w_1^{1/2} \Delta_1$ for all $j = 1, \dots, n_0$. \square

Estimating elastic full Procrustes means via Hermitian covariance smoothing

In the following, we provide additional details for three steps in our proposed elastic full Procrustes mean estimation algorithm. We commence with proposing a more efficient covariance estimation procedure for data with densely observed curves and continue with a discussion of conditional complex Gaussian processes in Proposition B1 underlying our estimation of length and optimal rotation of curves. Finally, we detail the warping alignment strategy proposed for the re-parameterization step.

Covariance estimation for densely observed curves: If curves y_1, \dots, y_n , are sampled densely enough, covariance estimation can be achieved computationally more efficient than by Hermitian covariance smoothing. In fact, for say $n_i > 1000$ samples per curve and m basis functions $\mathbf{f} = (f_1, \dots, f_m)^\top$ for each margin, setting up the joint $(\sum_{i=1}^n n_i^2) \times (m^2 \pm m)/2$ design matrices for tensor-product covariance smoothing may also cause working memory shortage. Using the notation of Section 2.2, we obtain a tensor-product covariance estimator $\hat{C}(s, t) = \mathbf{f}^\top(s) \hat{\Xi} \mathbf{f}(t)$ of the same form by setting $\hat{\Xi} = \frac{1}{n} \sum_{i=1}^n \hat{\boldsymbol{\vartheta}}_i \hat{\boldsymbol{\vartheta}}_i^\dagger$ to the empirical covariance matrix of complex coefficient vectors $\hat{\boldsymbol{\vartheta}}_i = (\hat{\vartheta}_{i1}, \dots, \hat{\vartheta}_{im})^\top \in \mathbb{C}^m$ of basis representations $y_i(t) \approx \sum_{k=1}^m \hat{\vartheta}_{ik} f_k(t)$ for $i = 1, \dots, n$. Partitioning the data into $\mathcal{N}_1 \cup \dots \cup \mathcal{N}_N = \{1, \dots, n\}$ subsets for computational efficiency (which might simply be given by $\mathcal{N}_i = \{i\}$), the estimators $\hat{\boldsymbol{\vartheta}}_i$ are fit by minimizing the penalized least-squares criterion

$$\text{PLS}(\boldsymbol{\vartheta}_{i\Re}, \boldsymbol{\vartheta}_{i\Im}) = \sum_{i \in \mathcal{N}_l} \sum_{j=1}^{n_i} |y_{ij} - \boldsymbol{\vartheta}_{i\Re}^\top \mathbf{f}(t_{ij}) - \mathbf{i} \boldsymbol{\vartheta}_{i\Im}^\top \mathbf{f}(t_{ij})|^2 + \eta \boldsymbol{\vartheta}_{i\Re}^\top \mathbf{P} \boldsymbol{\vartheta}_{i\Re} + \eta \boldsymbol{\vartheta}_{i\Im}^\top \mathbf{P} \boldsymbol{\vartheta}_{i\Im}$$

with $\boldsymbol{\vartheta}_{i\Re} = \Re(\boldsymbol{\vartheta}_i)$ and $\boldsymbol{\vartheta}_{i\Im} = \Im(\boldsymbol{\vartheta}_i)$, for $l = 1, \dots, N$. In principle, real and imaginary parts can be separately fit with the same smoothing parameter $\eta \geq 0$ in both parts to achieve rotation invariant penalization. As in Section 2.2, we use the `mgcv` framework for fitting (Wood, 2017) using restricted maximum likelihood (REML) estimation for η . To speed up computation, η can be estimated only on \mathcal{N}_1 and fixed for $l = 2, \dots, N$, or set to $\eta = 0$ if no measurement error is assumed or no penalization is desired. The residual variance yields a constant estimate for τ^2 . Using for instance `mgcv`'s “`gauss`” family, a smooth estimator $\hat{\tau}^2(t)$ could be obtained as well but is not detailed here.

Rotation and length estimation: A working normality assumption allows us to incorporate the estimated covariance structure of the data into estimation of inner products and quadratic terms underlying the length and optimal rotation of curves (Equation (B3) and (B4) in Proposition B1 iii). We provide required conditional expectations covering both the case of a positive white noise error variance $\tau^2(t) > 0$ and of no white noise error ($\tau^2(t) = 0$) for each time point t .

PROPOSITION B1 (CONDITIONAL GAUSSIAN PROCESS). Consider a random element Y in a complex Hilbert space \mathbb{H} of functions $\mathcal{T} \rightarrow \mathbb{C}$ defined on some set \mathcal{T} . Assume $Y = \sum_{k=1}^m Z_k e_k$ finitely generated with probability one from a finite set $\mathbf{e}(t) = (e_1(t), \dots, e_m(t))^\top$ of functions $e_k \in \mathbb{H}$ with regular Gramian $\mathbf{G} = \{\langle e_k, e_{k'} \rangle\}_{k, k'} \in \mathbb{C}^{m \times m}$ and with $\mathbf{Z} = (Z_1, \dots, Z_m)^\top$ following a complex symmetric multivariate normal distribution with mean zero and positive-definite covariance matrix $\mathbf{\Lambda}$. Let further denote ε an uncorrelated complex symmetric error process on \mathcal{T} with zero mean and variance function $\tau^2 : \mathcal{T} \rightarrow \mathbb{R}$. We consider a sequence of $n_* = n_+ + n_0$ points $t_1, \dots, t_{n_*} \in \mathcal{T}$ and values $y_1, \dots, y_{n_*} \in \mathbb{C}$ with $\tau^2(t_1), \dots, \tau^2(t_{n_+}) > 0$ and $\tau^2(t_{n_++1}), \dots, \tau^2(t_{n_++n_0}) = 0$, and write $\mathbf{E} = \{e_k(t_j)\}_{jk} = (\mathbf{E}_+^\top, \mathbf{E}_0^\top)^\top$ for the $n_* \times m$ design matrix of function evaluations subdivided into $\mathbf{E}_+ \in \mathbb{C}^{n_+ \times m}$ and $\mathbf{E}_0 \in \mathbb{C}^{n_0 \times m}$ containing the evaluations with positive and zero error variance, respectively, and analogously $\mathbf{y} = (y_1, \dots, y_{n_*})^\top = (\mathbf{y}_+^\top, \mathbf{y}_0^\top)^\top$ for the values and $\mathbf{T}_+ = \text{Diag}(\tau^2(t_1), \dots, \tau^2(t_{n_+}))$ for the diagonal $n_+ \times n_+$ noise covariance matrix. Let $r_0 = \text{rank}(\mathbf{E}_0)$ denote the rank of \mathbf{E}_0 and

$\mathbf{Q} = (\mathbf{M}, \mathbf{N})$ be an $m \times m$ Hermitian matrix such that \mathbf{M} is $m \times r_0$ and \mathbf{N} spans the null space of \mathbf{E}_0 . \mathbf{Q} is obtained, e.g., by the QR-decomposition $\mathbf{E}_0^\top = \mathbf{Q}\mathbf{R}$. By convention, \mathbf{N} and all other matrices are set to 0 if their rank is zero (i.e., if $m - r_0$, n_0 , or $n_+ = 0$, respectively). Conditioning on $Y(t_j) + \varepsilon(t_j) = \mathbf{Z}^\top \mathbf{e}(t_j) + \varepsilon(t_j) = y_j$ for $j = 1, \dots, n_*$ we obtain:

- i) By conditioning on $\mathbf{E}_0 \mathbf{Z} = \mathbf{y}_0$ in particular, $\mathbf{Z} = \mathbf{Z}_+ + \mathbf{z}_0$ is split into a random part $\mathbf{Z}_+ = \mathbf{N} \tilde{\mathbf{Z}}_+$ constrained to the linear sup-space $\text{span}(\mathbf{N})$ spanned by \mathbf{N} and a deterministic part $\mathbf{z}_0 = \mathbf{M} \left(\mathbf{M}^\dagger \mathbf{E}_0^\dagger \mathbf{E}_0 \mathbf{M} \right)^{-1} \mathbf{M}^\dagger \mathbf{E}_0^\dagger \mathbf{y}_0$. In fact, under the given assumptions $\mathbf{z}_0 = \mathbf{M} (\mathbf{M} \mathbf{E}_0)^{-\dagger} \mathbf{y}_0$ with probability one, but the generalized inverse is robust with respect to the case where $\mathbf{y}_0 \notin \text{span}(\mathbf{E}_0)$, i.e. where no measurement error is assumed but the curve cannot be exactly fit by the chosen basis.
- ii) $\tilde{\mathbf{Z}}_+$ follows a complex normal with covariance $\mathbf{S} = \left(\mathbf{N}^\dagger \left(\mathbf{E}_+^\dagger \mathbf{T}_+^{-1} \mathbf{E}_+ + \mathbf{\Lambda}^{-1} \right) \mathbf{N} \right)^{-1}$, mean $\hat{\mathbf{z}}_+ = \mathbf{N} \mathbf{S} \mathbf{N}^\dagger \left(\mathbf{E}_+^\dagger \mathbf{T}_+^{-1} (\mathbf{y}_+ - \mathbf{E}_+ \mathbf{z}_0) - \mathbf{\Lambda}^{-1} \mathbf{z}_0 \right)$ and zero pseudo-covariance.
- iii) For $x \in \mathbb{H}$ and $\mathbf{g}_x = (\langle e_1, x \rangle, \dots, \langle e_m, x \rangle)$, this provides conditional means

$$\hat{\mathbf{z}} = \mathbb{E}(\mathbf{Z} \mid Y(t_j) + \varepsilon(t_j) = y_j, j = 1, \dots, n_*) = \mathbf{M} \hat{\mathbf{z}}_+ + \mathbf{z}_0 \quad (\text{B2})$$

$$\mathbb{E}(\langle Y, x \rangle \mid Y(t_j) + \varepsilon(t_j) = y_j, j = 1, \dots, n_*) = \hat{\mathbf{z}}^\dagger \mathbf{g}_x \quad (\text{B3})$$

$$\mathbb{E}(\|Y\|^2 \mid Y(t_j) + \varepsilon(t_j) = y_j, j = 1, \dots, n_*) = \text{tr}(\mathbf{S} \mathbf{G}) + \hat{\mathbf{z}}^\dagger \mathbf{G} \hat{\mathbf{z}}. \quad (\text{B4})$$

$$\mathbb{E}(|\langle Y, x \rangle|^2 \mid Y(t_j) + \varepsilon(t_j) = y_j, j = 1, \dots, n_*) = \mathbf{g}_x^\dagger \mathbf{S} \mathbf{g}_x + \mathbf{g}_x \hat{\mathbf{z}}^\dagger \hat{\mathbf{z}} \mathbf{g}_x^\dagger. \quad (\text{B5})$$

Proof. The computation is analogous to the real case. Defining $\mathbf{Y} = (Y(t_1), \dots, Y(t_{n_*}))^\top$, i.e. $\mathbf{Y} = \mathbf{E} \mathbf{Z}$, and $\boldsymbol{\varepsilon} = (\varepsilon(t_1), \dots, \varepsilon(t_{n_*}))^\top$, the distribution of $\tilde{\mathbf{Z}} = \mathbf{Q}^\dagger \mathbf{Z} = (\mathbf{M}^\dagger \mathbf{Z}, \mathbf{N}^\dagger \mathbf{Z})^\dagger = (\tilde{\mathbf{Z}}_0^\dagger, \tilde{\mathbf{Z}}_+^\dagger)^\dagger$ conditional on $\mathbf{Y} + \boldsymbol{\varepsilon} = \mathbf{y}$ has a density proportional to

$$\begin{aligned} p_{\tilde{\mathbf{Z}}}(\tilde{\mathbf{z}} \mid \mathbf{Y} + \boldsymbol{\varepsilon} = \mathbf{y}) &\propto p_{\tilde{\mathbf{Z}}, \mathbf{Y} + \boldsymbol{\varepsilon}}(\tilde{\mathbf{z}}, \mathbf{Y} + \boldsymbol{\varepsilon}) 1_{\{\mathbf{M}^\dagger \mathbf{z}_0\}}(\tilde{\mathbf{z}}_0) \propto p_{\mathbf{Z}, \boldsymbol{\varepsilon}}(\mathbf{Q} \tilde{\mathbf{z}}, \mathbf{y} - \mathbf{E} \mathbf{Q} \tilde{\mathbf{z}}) 1_{\{\mathbf{M}^\dagger \mathbf{z}_0\}}(\tilde{\mathbf{z}}_0) \\ &\propto \exp \left(-\frac{1}{2} \left(\tilde{\mathbf{z}}_+^\dagger \mathbf{N}^\dagger \mathbf{\Lambda}^{-1} \mathbf{N} \tilde{\mathbf{z}}_+ + \mathbf{z}_0^\dagger \mathbf{\Lambda}^{-1} \mathbf{z}_0 \right) - \Re \left(\tilde{\mathbf{z}}_+^\dagger \mathbf{N}^\dagger \mathbf{\Lambda}^{-1} \mathbf{z}_0 \right) \right) \times \\ &\quad \exp \left(-\frac{1}{2} (\mathbf{y}_+ - \mathbf{E}_+ \mathbf{z}_0 - \mathbf{E}_+ \mathbf{N} \tilde{\mathbf{z}}_+)^{\dagger} \mathbf{T}_+^{-1} (\mathbf{y}_+ - \mathbf{E}_+ \mathbf{z}_0 - \mathbf{E}_+ \mathbf{N} \tilde{\mathbf{z}}_+) \right) 1_{\{\mathbf{M}^\dagger \mathbf{z}_0\}}(\tilde{\mathbf{z}}_0) \\ &\propto \exp \left(-\frac{1}{2} \tilde{\mathbf{z}}_+^\dagger \underbrace{\mathbf{N}^\dagger \left(\mathbf{\Lambda}^{-1} + \mathbf{E}_+^\dagger \mathbf{T}_+^{-1} \mathbf{E}_+ \right) \mathbf{N}}_{=\mathbf{S}^{-1}} \tilde{\mathbf{z}}_+ - \Re \left(\tilde{\mathbf{z}}_+^\dagger \mathbf{N}^\dagger \mathbf{\Lambda}^{-1} \mathbf{z}_0 \right) \right) \\ &\quad + \Re \left(\tilde{\mathbf{z}}_+^\dagger \mathbf{N}^\dagger \mathbf{E}_+^\dagger \mathbf{T}_+^{-1} (\mathbf{y}_+ - \mathbf{E}_+ \mathbf{z}_0) \right) 1_{\{\mathbf{M}^\dagger \mathbf{z}_0\}}(\tilde{\mathbf{z}}_0) \\ &\propto \exp \left(-\frac{1}{2} \left(\tilde{\mathbf{z}}_+ - \mathbf{S} \mathbf{N}^\dagger \left(\mathbf{E}_+^\dagger \mathbf{T}_+^{-1} (\mathbf{y}_+ - \mathbf{E}_+ \mathbf{z}_0) - \mathbf{\Lambda}^{-1} \mathbf{z}_0 \right) \right)^\dagger \mathbf{S}^{-1} \right. \\ &\quad \left. \left(\tilde{\mathbf{z}}_+ - \mathbf{S} \mathbf{N}^\dagger \left(\mathbf{E}_+^\dagger \mathbf{T}_+^{-1} (\mathbf{y}_+ - \mathbf{E}_+ \mathbf{z}_0) - \mathbf{\Lambda}^{-1} \mathbf{z}_0 \right) \right) \right) 1_{\{\mathbf{M}^\dagger \mathbf{z}_0\}}(\tilde{\mathbf{z}}_0) \\ &= \exp \left(-\frac{1}{2} \left(\tilde{\mathbf{z}}_+ - \mathbf{N}^\dagger \hat{\mathbf{z}}_+ \right)^\dagger \mathbf{S}^{-1} \left(\tilde{\mathbf{z}}_+ - \mathbf{N}^\dagger \hat{\mathbf{z}}_+ \right) \right) 1_{\{\mathbf{M}^\dagger \mathbf{z}_0\}}(\tilde{\mathbf{z}}_0). \end{aligned}$$

which shows i) and ii). In iii), (B2) and (B3) follow directly by linearity, B4) from variance decomposition (omitting conditions for brevity):

$$\begin{aligned} \mathbb{E}(\|Y\|^2) &= \mathbb{E} \left(\left\langle \sum_{k=1}^m Z_k e_k, \sum_{k=1}^m Z_k e_k \right\rangle \right) = \mathbb{E}(\mathbf{Z}^\dagger \mathbf{G} \mathbf{Z}) = \mathbb{E}(\text{tr}(\mathbf{Z} \mathbf{Z}^\dagger \mathbf{G})) \stackrel{\text{linearity}}{=} \text{tr}(\mathbb{E}(\mathbf{Z} \mathbf{Z}^\dagger) \mathbf{G}) \\ &= \text{tr} \left(\left(\text{Var}(\mathbf{Z}) + \mathbb{E}(\mathbf{Z}) \mathbb{E}(\mathbf{Z})^\dagger \right) \mathbf{G} \right) \stackrel{\text{ii)}}{=} \text{tr}(\mathbf{S} \mathbf{G}) + \hat{\mathbf{z}}^\dagger \mathbf{G} \hat{\mathbf{z}}. \end{aligned}$$

The computation for (B5) is analogous. □

Warping alignment: Generally, we consider it advisable to base warping alignment of the i th curve directly on its original SRV-evaluations $q_{i1}^{[h]}, \dots, q_{in_i}^{[h]}$ but, when considerable measurement error presents an issue, it might also be useful to employ a smoothed reconstruction $\tilde{q}_i : [0, 1] \rightarrow \mathbb{C}$ of the SRV-transform in the assumed basis. Based on the working normality assumption used also for length and rotation estimation, such a reconstruction is obtained as $\tilde{q}_i^{[h]}(t) = (\hat{\mathbf{z}}_i^{[h]} / \|\hat{\mathbf{z}}_i^{[h]}\|)^\top \hat{\mathbf{e}}^{[h]}(t)$ with $\hat{\mathbf{z}}_i^{[h]} = (\hat{z}_{i1}^{[h]}, \dots, \hat{z}_{im}^{[h]})^\top$ the predicted score vector for the eigenbasis $\hat{\mathbf{e}}^{[h]} = (\hat{e}_1^{[h]}, \dots, \hat{e}_m^{[h]})^\top$.

Following Steyer et al. (2021), warping alignment to $\hat{\mu}^{[h]}$ is conducted using another, polygonal approximation of the curve given by a piece-wise constant approximation $\hat{q}_i^{[h]} \in \mathbb{L}^2([0, 1], \mathbb{C})$ of $\tilde{q}_i^{[h]}$. With a hyper-parameter $\rho \in [0, 1]$, we control the balance between original $q_{ij}^{[h]}$ (for $\rho = 0$) and smoothed reconstruction \tilde{q}_i (for $\rho = 1$) and set $\hat{q}_{ij}^{[h]} = \hat{u}_i^{[h]} \left(\rho \tilde{q}_i^{[h]}(t_{ij}^{[h]}) + (1 - \rho) q_{ij}^{[h]} \right)$ at nodes $s_{i0}^{[h]} = 0, s_{ij}^{[h]} = 2t_{ij}^{[h]} - s_{ij-1}^{[h]}, j = 1, \dots, n_i$. This defines $\hat{q}_i^{[h]}(t) = \sum_{j=1}^{n_i} \hat{q}_{ij}^{[h]} 1_{[s_{ij-1}^{[h]}, s_{ij}^{[h]}]}(t)$ already rotated by $\hat{u}_i^{[h]}$.

Warping alignment to $\hat{\mu}^{[h]}$ is achieved for $i = 1, \dots, n$ by finding an optimal $\hat{q}_i^* \in \mathbb{L}^2([0, 1], \mathbb{C})$ with

$$\|\hat{q}_i^* - \hat{\psi}^{[h]}\| \leq \|\hat{q}_i^{[h]} \circ \gamma^{\gamma^{1/2}} - \hat{\psi}^{[h]}\| \quad \text{for all } \gamma \in \Gamma \quad (\text{B6})$$

where the polygon approximation yields a practically feasible optimization problem and has proven suitable for sparse/irregular curves (Steyer et al., 2021). As shown by Steyer et al. (2021), the optimizers of (B6) have the form $\hat{q}_i^*(t) = \sum_{j=1}^{n_i} w_i(t) \hat{q}_{ij}^{[h]} 1_{[s_{ij-1}^{[h+1]}, s_{ij}^{[h+1]}]}(t)$ almost-everywhere, where, denoting $a_+ = \max\{a, 0\}$ for $a \in \mathbb{R}$, the functions $w_i : [0, 1] \rightarrow \mathbb{R}$ are given by $w_i^2(t) = (s_{ij}^{[h]} - s_{ij-1}^{[h]}) \Re \left(\psi^{[h]}(t)^\dagger \hat{q}_{ij}^{[h]} \right)_+^2 / \int_{s_{ij-1}^{[h+1]}}^{s_{ij}^{[h+1]}} \Re \left(\psi^{[h]}(t)^\dagger \hat{q}_{ij}^{[h]} \right)_+^2 dt$ for $t \in [s_{ij-1}^{[h+1]}, s_{ij}^{[h+1]})$, and fully determined by the warped time points

$$(s_{i1}^{[h+1]}, \dots, s_{in_i-1}^{[h+1]}) = \arg \max_{0=s_{i0} \leq \dots \leq s_{in_i}=1} \sum_{j=1}^{n_i} \left((s_{ij}^{[h]} - s_{ij-1}^{[h]}) \int_{s_{ij-1}^{[h+1]}}^{s_{ij}^{[h+1]}} \Re \left(\psi^{[h]}(t)^\dagger \hat{q}_{ij}^{[h]} \right)_+^2 dt \right)^{1/2}.$$

If $s_{ij}^{[h+1]} = s_{ij-1}^{[h+1]}$ for some j , there is a minimizing sequence of functions of the form given for \hat{q}_i^* . After optimization over the $s_{ij}^{[h]}$ with R package `elasdics` (Steyer, 2021), we set new $t_{ij}^{[h+1]} = (s_{ij-1}^{[h+1]} + s_{ij}^{[h+1]})/2$ and $q_{ij}^{[h+1]} = w_j^* q_{ij}^{[h]}$ with $w_j^* = (s_{ij}^{[h]} - s_{ij-1}^{[h]})^{1/2} (s_{ij}^{[h+1]} - s_{ij-1}^{[h+1]})^{-1/2}$ for $s_{ij}^{[h+1]} > s_{ij-1}^{[h+1]}$ and omit double time points for $j = 1, \dots, n_i$. The chosen time-points hereby approximate $t_{ij}^{[h+1]} \approx t_{ij}^* \in (s_{ij}^{[h+1]}, s_{ij-1}^{[h+1]})$ with $w_i(t_{ij}^*) = w_{ij}^*$ existing by the Mean Value Theorem.

REFERENCES

- BRUVERIS, M. (2016). Optimal reparametrizations in the square root velocity framework. *SIAM Journal on Mathematical Analysis* **48**, 4335–4354.
- CEDERBAUM, J. (2018). *sparseFLMM: Functional Linear Mixed Models for Irregularly or Sparsely Sampled Data*. R package version 0.2-2.
- CEDERBAUM, J., SCHEIPL, F. & GREVEN, S. (2018). Fast symmetric additive covariance smoothing. *Computational Statistics & Data Analysis* **120**, 25–41.
- DAVIDSON, L. (2006). Comparing tongue shapes from ultrasound imaging using smoothing spline analysis of variance. *The Journal of the Acoustical Society of America* **120**, 407–415.
- DRYDEN, I. L., LE, H., PRESTON, S. P. & WOOD, A. T. (2014). Mean shapes, projections and intrinsic limiting distributions. *Journal of Statistical Planning and Inference*, 25–32.
- DRYDEN, I. L. & MARDIA, K. V. (2016). *Statistical Shape Analysis: With Applications in R*. John Wiley & Sons.
- GREVEN, S. & SCHEIPL, F. (2017). A general framework for functional regression modelling (with discussion and rejoinder). *Statistical Modelling* **17**, 1–35 and 100–115.
- HAPP, C. & GREVEN, S. (2018). Multivariate functional principal component analysis for data observed on different (dimensional) domains. *Journal of the American Statistical Association* **113**, 649–659.
- HOOLE, P. (1999). On the lingual organization of the german vowel system. *The Journal of the Acoustical Society of America* **106**, 1020–1032.

- HSING, T. & EUBANK, R. (2015). *Theoretical foundations of functional data analysis, with an introduction to linear operators*. John Wiley & Sons.
- HUCKEMANN, S. F. (2012). On the meaning of mean shape: manifold stability, locus and the two sample test. *Annals of the Institute of Statistical Mathematics* **64**, 1227–1259.
- ISKAROUS, K. (2005). Patterns of tongue movement. *Journal of Phonetics* **33**, 363–381.
- KENT, J. T. (1994). The complex bingham distribution and shape analysis. *Journal of the Royal Statistical Society: Series B (Methodological)* **56**, 285–299.
- NEESER, F. D. & MASSEY, J. L. (1993). Proper complex random processes with applications to information theory. *IEEE transactions on information theory* **39**, 1293–1302.
- PICINBONO, B. (1996). Second-order complex random vectors and normal distributions. *IEEE Transactions on Signal Processing* **44**, 2637–2640.
- RAMSAY, J. O. & SILVERMAN, B. W. (2005). *Functional Data Analysis*. Springer New York.
- REISS, P. T. & XU, M. (2020). Tensor product splines and functional principal components. *Journal of Statistical Planning and Inference* **208**, 1–12.
- RYNNE, B. & YOUNGSON, M. A. (2007). *Linear functional analysis*. Springer Science & Business Media.
- SRIVASTAVA, A., KLASSEN, E., JOSHI, S. H. & JERMYN, I. H. (2011). Shape analysis of elastic curves in Euclidean spaces. *IEEE Transactions on Pattern Analysis and Machine Intelligence* **33**, 1415–1428.
- SRIVASTAVA, A. & KLASSEN, E. P. (2016). *Functional and Shape Data Analysis*. Springer-Verlag.
- STEYER, L. (2021). *elasdics: Elastic Analysis of Sparse, Dense and Irregular Curves*. R package version 0.1.3.
- STEYER, L., STÖCKER, A. & GREVEN, S. (2021). Elastic analysis of irregularly or sparsely sampled curves. *arXiv preprint arXiv:2104.11039*.
- STONE, M., DAVIS, E. P., DOUGLAS, A. S., AIVER, M. N., GULLAPALLI, R., LEVINE, W. S. & LUNDBERG, A. J. (2001). Modeling tongue surface contours from cine-mri images.
- WOOD, S. (2017). *Generalized Additive Models: An Introduction with R*. Chapman and Hall/CRC, 2nd ed.
- WOOD, S. N., PYA, N. & SÄFKEN, B. (2016). Smoothing parameter and model selection for general smooth models. *Journal of the American Statistical Association* **111**, 1548–1563.
- YAO, F., MÜLLER, H. & WANG, J. (2005). Functional data analysis for sparse longitudinal data. *Journal of the American Statistical Association* **100**, 577–590.
- ZIEZOLD, H. (1977). On expected figures and a strong law of large numbers for random elements in quasi-metric spaces. In *Transactions of the Seventh Prague Conference on Information Theory, Statistical Decision Functions, Random Processes and of the 1974 European Meeting of Statisticians*. Springer.